

UCUENCA

Facultad de Ingeniería

Maestría en Hidrología, Mención Ecohidrología

Factors controlling the temporal variability of streamflow transit times in tropical alpine catchments

Trabajo de titulación previo a la obtención del título de Magíster en Hidrología, Mención Ecohidrología

Autora:

Karina Marlene Larco Erazo

CI: 1719377382

Correo electrónico: karynina3@gmail.com

Director:

Giovanny Mauricio Mosquera Rojas

CI: 0104450911

Cuenca-Ecuador

15-junio-2022

Resumen:

El tiempo medio de tránsito (MTT) del agua es un descriptor esencial de la generación de caudales y del almacenamiento de agua en las cuencas. La investigación sobre cómo fluctúan los MTTs a lo largo del tiempo y los factores que influyen en dicha variación es limitada. En este estudio se presentan datos isotópicos estables quincenales en la precipitación y el caudal, junto con registros diarios de la cantidad de precipitación, caudal e información climatológica. Los datos se recogieron durante un período de 8 años en un sistema anidado de 8 cuencas alpinas tropicales en el Observatorio Ecohidrológico de Zhurucay, en el sur de Ecuador, situado a una altitud de 3400 a 3900 m s.n.m. Los datos isotópicos se utilizaron para investigar la variabilidad temporal de los MTTs de los caudales estimados utilizando períodos anuales y una ventana móvil de 1 mes (es decir, 81 MTTs calculados anualmente por cuenca). Los factores que controlan la variabilidad temporal de los MTTs se identificaron mediante modelos de regresión lineal simple y múltiple entre los MTTs estimados y las variables hidrometeorológicas. Los resultados revelan que los MTT de los caudales en todas las cuencas fueron cortos (<1 año) y variaron poco entre ellas (191.30 ± 47.10 días), lo que sugiere que un lapso de tiempo anual para estimar la variabilidad temporal de los MTTs es apropiado. Una combinación de variables hidrometeorológicas (precipitación, caudal y coeficiente de escorrentía) durante períodos anteriores de hasta 1 año controlan la variabilidad temporal de los MTTs entre cuencas. En general, estos resultados apuntan a la prevalencia de condiciones de estado estacionario en el sistema hidrológico investigado. Nuestro estudio es clave para proporcionar información sobre los factores que controlan la variabilidad temporal de los MTTs de los caudales en las cuencas tropicales, superando las limitaciones de datos de las investigaciones anteriores. También proporciona un aumento en el conocimiento basado en procesos hidrológicos de las cuencas del Páramo alto andino, con implicaciones significativas para una mejor gestión del suministro de agua.

Palabras claves: Tiempos de tránsito. Isótopos estables. Hidrología de trazadores. Páramo. Variación temporal. Estado estable.

Abstract:

The mean transit time (MTT) of water is an essential descriptor of streamflow generation and catchment water storage. Research on how MTTs fluctuate over time and the variables influencing such variation is limited. In this study bi-weekly stable isotopic data in precipitation and streamflow are presented, together with daily records of precipitation amount, streamflow, and climatological information. The data were collected over an 8-year period in a nested system of 8 tropical alpine catchments in the Zhurucay Ecohydrological Observatory in southern Ecuador, situated at an elevation of 3400 to 3900 m a.s.l. Isotopic data were used to investigate the temporal variability of streamflow MTTs estimated using yearly periods and a 1-month moving window (i.e., 81 yearly calculated MTTs per catchment). The factors controlling the temporal variability of MTTs were identified using simple and multiple linear regression models between estimated MTTs and hydrometeorological variables. Results reveal that streamflow MTTs at all catchments were short (<1 year) and varied little among catchments (191.30 ± 47.10 days), suggesting that a yearly time span for estimating the temporal variability of MTTs is appropriate. A combination of hydrometeorological variables (i.e., precipitation, streamflow, and runoff coefficient) over antecedent periods up to 1 year was found to control MTT temporal variability among catchments. Overall, these findings point to the prevalence of steady-state conditions in the investigated hydrological system. Our study is key to provide insights into the factors controlling the temporal variability of streamflow MTT in tropical catchments, overcoming data limitations of past investigations. It also provides an increase in the process-based knowledge of the hydrology of high Andean Páramo catchments, with significant implications for improved water supply management.

Keywords: Transit time. Stables isotopes. Tracer hydrology. Páramo. Temporal variability. Steady-state.

Índice del Trabajo

1. Introduction	10
2. Materials and methods.....	12
2.1. Study area.....	12
2.2. Hydrometeorological information.....	13
2.3. Collection of water samples and laboratory analysis	14
2.4. Mean transit time modelling	14
2.5. Evaluation of factors controlling the temporal variability of MTTs	17
3. Results.....	19
3.1. Hydrometeorological and isotopic characterization	19
3.2. Mean transit time modelling	21
3.3. Identification of factors controlling the temporal variability of MTTs	24
4. Discussion.....	28
4.1. Mean Transit Time Modelling	28
4.2. Identification of factors controlling temporal variability of MTTs	29
5. Conclusion	32
6. References	33
S. Supplementary material	41
S1. Simple Linear Regression.....	41
S2. Multiple Linear Regressions.....	47

Índice de Figuras

Figure 1. Nested system of catchments (M1-M8) and the distribution of rain gauges (P1-P4) in the Zhurucay Ecohydrological Observatory located in southern Ecuador..... 13

Figure 2. Time series of hydrometeorological and stable isotopic data in the period May 2011 - December 2018. **(a)** Daily precipitation and streamflow; **(b)** daily evapotranspiration, and **(c)** $\delta^{18}\text{O}$ isotopic composition of precipitation and streamflow of catchment M6 collected at event-based (sub-daily) and monthly frequency (the triangles show the $\delta^{18}\text{O}$ isotopic data collected during rainfall events). The white/light gray shaded areas indicate yearly periods. 19

Figure 3. Box plots of the hydrometric variables for each of the studied micro-catchments (M1-M8) during the period May 2011 - December 2018 using a monthly moving window. The box represents the median and the interquartile range, the whiskers represent 1.5 times the interquartile range, and the black dots represent the outliers. Abbreviations: **Qmn** mean streamflow; **Qmd** median streamflow; **Qmx** maximum streamflow; **Qmin** minimum streamflow; **Q₁₀**, **Q₂₀**, **Q₃₀**...., **Q₉₀** streamflow rates as the frequency of non-exceedance; **Pmn** mean precipitation; **Pmd** median precipitation; **RC** runoff coefficient. 21

Figure 4. Observed and simulated $\delta^{18}\text{O}$ streamflow isotopic composition during the period May 2011 - December 2018 for catchments: **(a)** M3, **(b)** M6, and **(c)** M7. The green shaded area represents the 5-95% confidence limits based on the MTT parameter values used in the simulations. The white/light gray shaded areas indicate yearly periods. 22

Figure 5. Yearly estimated MTTs using a monthly moving window for catchment M6 (gray bars) during the period May 2011 - December 2018. The MTTs correspond to the parameter value that yielded the highest KGE value during the simulations (blue line). The dashed red line represents the KGE value of 0.45 considered in this study as a threshold between good (values above) and poor (values below) model predictions. The figure only shows the beginning date of each yearly moving window (i.e., the MTT and KGE values corresponding to August 2014 were obtained for the simulation period August 2014 - July 2015). 23

Figure 6. Box plots of the **(a)** yearly estimated MTTs using a monthly moving window for catchments M1-M8, and **(b)** their corresponding KGE values. The box represents the median and interquartile range, the whiskers represent 1.5 times the interquartile range, and the black dots represent the outliers. The red crosses represent the average of the distributions of MTT and KGE values. The dashed red line in subplot **(b)** represents the KGE value of 0.45 considered in this study as a threshold between good (values above) and poor (values below) model predictions. 24

Figure 7. Multiple linear regression models for micro catchment M6 for the period May 2011 - December 2018 using hydrological and meteorological variables as predictors. **A1** to **A5** represents different models after incorporation of the explanatory variables. The number next to the hydrological variable indicates the corresponding moving window. Abbreviations: **RC** runoff coefficient; **Qmin** minimum streamflow; **Qmx** maximum streamflow; **Pcum** cumulative precipitation. The dashed line shows the 1:1 ratio relation. 25

Índice de Tablas

Table 1. Summary statistics of the $\delta^{18}\text{O}$ isotopic composition in precipitation (P1) and streamflow (M1-M8) collected during the period May 2011 - May 2018. 20

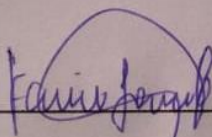
Table 2. Factors controlling the temporal variation of MTTs using multiple linear regression (MLR) with their respective statistical metrics for catchments M1-M8 during the period May 2011 - December 2018. 27

Cláusula de licencia y autorización para publicación en el Repositorio
Institucional

Yo, Karina Marlène Larco Erazo en calidad de autor y titular de los derechos morales y patrimoniales del trabajo de titulación **“Factors controlling the temporal variability of streamflow transit times at tropical alpine catchments”**, de conformidad con el Art. 114 del CÓDIGO ORGÁNICO DE LA ECONOMÍA SOCIAL DE LOS CONOCIMIENTOS, CREATIVIDAD E INNOVACIÓN reconozco a favor de la Universidad de Cuenca una licencia gratuita, intransferible y no exclusiva para el uso no comercial de la obra, con fines estrictamente académicos.

Asimismo, autorizo a la Universidad de Cuenca para que realice la publicación de este trabajo de titulación en el repositorio institucional, de conformidad a lo dispuesto en el Art. 144 de la Ley Orgánica de Educación Superior.

Cuenca, 15 de junio de 2022



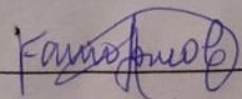
Karina Marlène Larco Erazo

171937738-2

Cláusula de Propiedad Intelectual

Yo, Karina Marlene Larco Erazo, autor del trabajo de titulación **“Factors controlling the temporal variability of streamflow transit times at tropical alpine catchments”**, certifico que todas las ideas, opiniones y contenidos expuestos en la presente investigación son de exclusiva responsabilidad de su autor.

Cuenca, 15 de junio de 2022



Karina Marlene Larco Erazo

171937738-2

DEDICATORIA

A Dios y mi familia por ser y siempre estar.

AGRADECIMIENTOS

A mi familia, mi razón de ser, por su amor, consejos y apoyo. A mis amigas y hermanas de vida, porque a pesar de la distancia el cariño sigue siendo infinito. A mis amigos en Cuenca, que me hicieron sentir como en casa. Y a mis profesores por acompañarme en el camino. En especial a mis profesores Giovanny Mosquera y Patricio Crespo, sin ellos no hubiera sido lo mismo.

1. Introduction

One of the most common catchment descriptors in hydrologic studies is the mean transit time (MTT) of streamflow. MTT is defined as the mean age of water that entered a catchment during previous precipitation events at the time of exit at an outlet point (i.e., streams, springs, soils; McGuire & McDonnell, 2006). This hydrological descriptor contains information about water storage and the flow paths water follows in a catchment (McGuire & McDonnell, 2006). The MTT of stream water can also help to better understand catchment biogeochemical processes (Burns et al., 2003). Hence, the MTT is a key hydrological parameter for risk assessment, contaminant remediation, land-use change, climate change, and improved management of water resources (Landon, Delin, Komor, & Regan, 2000; Nystrom, 1985; Turner et al., 2006).

The MTT can be calculated by modeling the relationship between input and output signals of conservative tracers such as water stable isotopes (^2H and ^{18}O ; McGuire & McDonnell 2006) or chloride (Kirchner, Tetzlaff, & Soulsby, 2010). Among the most common methods to estimate the MTT of water are the lumped convolution approach (LCA), the Fourier method, and the sine save method (Bennett, Rinaldo, & Botter, 2015). These methods take advantage of the damping of the isotopic composition of streamflow concerning the temporal variation of the isotopic composition of precipitation. The application of these methods could be difficult due to a range of uncertainties caused by the high spatial and temporal variability of the isotopic composition of water, the unavailability of long-term tracer records, and the low sampling frequency caused by financial and logistical constraints (Hrachowitz, Soulsby, Tetzlaff, Dawson, et al., 2009; McGuire & McDonnell, 2006). Notwithstanding, the study of MTT is crucial, since it enables a better understanding of the runoff generation process and the hydrological behavior of catchments.

MTTs vary in time as a result of seasonal and annual changes in hydrometeorological conditions (Birkel et al., 2016; Hrachowitz, Soulsby, Tetzlaff, Dawson, et al., 2009; Ma & Yamanaka, 2016). Therefore, understanding such temporal variation and its controlling factors is relevant to grasp the change in hydrological behavior over time of a given catchment. To date, most of the studies investigating the temporal variability of streamflow MTT have been conducted in temperate regions. For example, Hrachowitz et al. (2009) applied a moving window approach to estimate the variability of streamflow MTTs over 8 years in two small catchments ($\sim 1 \text{ km}^2$) in the Scottish Highlands. These authors found that the MTT temporal variability was influenced by precipitation amount. Applying a similar approach over 10 years, Ma & Yamanaka (2016) concluded that the temporal variation of MTT was similar for five temperate catchments (268-2173 km^2) in central Japan despite differences in slope, geology, and soil type. These authors reported that the estimated MTTs were longer during drier periods than during wetter periods, and mainly controlled by geology. Another investigation was carried out at a boreal catchment in north Sweden (0.47 km^2) using a 10-year isotopic data record (Peralta-Tapia et al., 2016). The authors determined a strong correlation between annual rainfall and MTTs during snow-free periods. In another study conducted in 4 catchments

in southeast Australia (8.7-323 km²) using 3 years of data, MTTs were found to be correlated with runoff coefficient (Cartwright et al., 2020).

In a tropical setting, Birkel et al. (2016) investigated the temporal variability of streamflow MTTs in a humid forested catchment (30 km²) in Costa Rica. These authors applied a lumped convolution model to a short-term isotopic tracer dataset (2-years) using a monthly moving window to estimate streamflow MTTs over 4-month time spans. Even though this study is, to our knowledge, the only one until today that investigated the temporal variability of MTTs in the tropics, the reported MTTs presented large uncertainties since many of the estimated MTTs were longer than the data records used for model calibration. This is most likely because the short time spans used to estimate the MTTs (<1 hydrologic year) violate the steady-state assumptions of the applied lumped convolution model (Mcguire & McDonnell, 2006). Based on those potentially biased MTT estimates, the reported finding of this research was that wind direction was the most important climatic variable influencing the temporal variability of MTTs.

Considering the very limited information on the temporal variability of MTTs in the tropics, the factors controlling it, and the large uncertainties of past studies primarily due to data limitations, filling this knowledge gap is an essential for achieving improved water resources management in tropical montane regions. To this end, we took advantage of a unique long-term tracer dataset in precipitation and streamflow collected over 8 years across 8 nested tropical alpine (Páramo) catchments in Southern Ecuador with the following objectives:

- 1) To estimate the temporal variability of MTTs across a nested system of tropical alpine catchments; and
- 2) To identify the hydrometeorological conditions that control the temporal variability of MTTs across the catchments, if any.

It is believed that the results obtained by this research are of crucial importance to better understand how the hydrological behavior of catchments varies over time, as the basis for the development of proper and efficient water conservation and management practices in the tropics.

2. Materials and methods

2.1. Study area

The study site is the Zhurucay Ecohydrological Observatory (ZEO) ($3^{\circ}4'S$, $79^{\circ}14'W$) located at the western slope of the Andean mountain range in southern Ecuador (Fig. 1). The observatory has a drainage area of 7.53 km^2 with an elevation ranging between 3505-3900 m a.s.l. ZEO is located in a tropical alpine (Páramo) ecosystem. The local climate is primarily influenced by continental air masses stemming from the Amazon basin, which originate mainly in the Atlantic Ocean (Esquivel et al., 2019). Annual precipitation shows low seasonality and is mainly composed of drizzle (Padrón et al., 2015). According to these authors, the wettest period lasts from March to May and the less wet period from August to October. At 3780 m.a.s.l., mean annual precipitation is 1345 mm, mean annual temperature is 6°C , mean relative humidity is 93.6% (Córdova et al., 2015), and the solar radiation is $4942\text{ MJ m}^{-2}\text{ g/year}$ (Carrillo-Rojas et al., 2019). Annual actual evapotranspiration is 622 mm (Ochoa-Sánchez, Crespo, Carrillo-Rojas, Sucozhañay, & Céller, 2019).

The geomorphology at the study site is U-shaped with an average slope of 17%, as a result of glacial activity (Mosquera et al., 2015). The geology is compacted and dominated by Quimsacocha and Turi formations, characterized by volcanic rock deposits compacted during the glacial activity of the last Ice Age (Coltorti & Ollier, 2000). Both formations date from the Late Miocene (Pratt, Figueira, & Flores, 1997). Lithology in the Quimsacocha formation is composed of basaltic flows with plagioclases, feldspars, and andesitic pyroclasts, whereas the Turi formation is composed of tuffaceous andesitic breccias, conglomerates, and horizontally stratified sands (Hungerbühler et al., 2002).

The main soil types in Zhurucay are classified as Andosols and Histosols (IUSS Working Group WRB, 2015), formed by the accumulation of volcanic ash in combination with the humid-cold climate conditions (Quichimbo et al., 2012). These soils of volcanic origin present a high content of organic matter, low bulk density, and high-water retention capacity, low pH, and low phosphorus availability (Buytaert, Deckers, & Wyseure, 2006; Marín et al., 2018). Andosols cover approximately 70% of the ZEO and are mainly located on the hillslopes, whereas the Histosols cover the remaining area and are mostly found at valley bottoms and flat areas (Mosquera et al., 2015). The vegetation type and the spatial distribution of the soils are highly correlated. Andosols are mainly covered by tussock grasses (*Calamagrostis* sp) and Histosols are associated with the presence of cushion plants (*Plantago rigida*, *Xenophyllum humile*, and *Azorella* spp.) which grow in the valley bottoms in permanent wet zones, known as Andean wetlands. A small area (5%) of ZEO is covered by *Polylepis* and pine forests. Land use and management are limited to non-intensive livestock at the lower part of the observatory.

UCUENCA

2.2. Hydrometeorological information

A nested monitoring scheme was used for the collection of water level data at seven tributary micro-catchments (M1-M7) and the outlet of the ZEO (M8; Fig. 1). Each catchment (M1-M7) had a V-notch weir at its outflow, and the M8 catchment had a rectangular weir at its outlet to measure discharge. A Schlumberger DI500 water-level sensor (Kent, WA, USA) with an accuracy of ± 5 mm was installed in each catchment. The Kindsvater-Shen Equation (U.S. Bureau of Reclamation, 2001) was used to convert water levels into discharge (Moore, 2004). Four Texas Electronics rain gauge tipping buckets TE-525MM (Dallas, TX, USA) were used to record precipitation with a resolution of 0.1 mm. Water level and precipitation amount were recorded at 5-min intervals from May 2011 to December 2018. The Thiessen Polygon Method was used to estimate precipitation amounts at each of the study catchments using the data from the rain gauges.

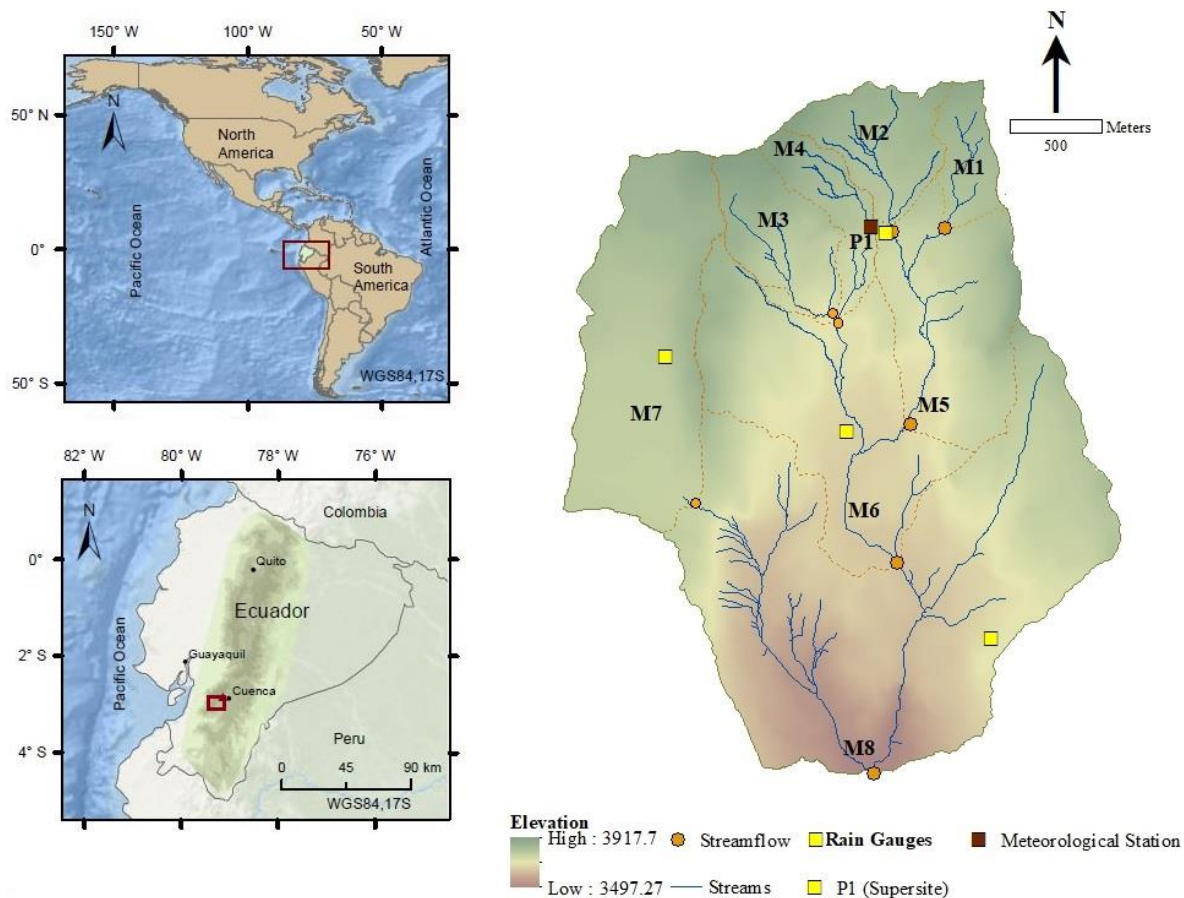


Figure 1. Nested system of catchments (M1-M8) and the distribution of rain gauges (P1-P4) in the Zhurucay Ecohydrological Observatory located in southern Ecuador.

Meteorological variables were monitored using a Campbell Scientific meteorological station (Logan, UT, USA), which was placed at the same location where rain gauge P1 is located (Fig. 1). Air temperature and relative humidity were measured with a CS-215 probe, with an accuracy of $\pm 0.3^{\circ}\text{C}$ for temperature and $\pm 2\%$ for relative humidity. Wind speed was recorded with Met-One 034B Winset anemometer with an accuracy of $\pm 0.11\text{m}^*\text{s}^{-1}$ and solar radiation was recorded with an Apogee CS300 pyranometer with an accuracy of $\pm 5\%$. Meteorological variables were also collected at 5-min intervals during the period from May 2011 to December 2018. These data were used to estimate daily reference evapotranspiration with the FAO-56 Penman-Monteith equation (Allen et al., 1998).

2.3. Collection of water samples and laboratory analysis

Streamflow and precipitation water samples for isotopic analysis were collected from May 2011 to December 2018. During this period the samples were collected at an event-based (sub-daily) to biweekly frequency, except in 2016 when samples were collected monthly. Grab samples were collected directly from the streams at the same locations where water levels were measured (M1-M8; Fig. 1). Precipitation samples were collected using a circular funnel (16 cm of diameter) connected to a glass bottle of 1000 mL at P1 (Fig. 1). The glass bottle was covered with aluminum foil for insulation of direct solar radiation to prevent isotopic fractionation by evaporation. A sphere of 4 cm of diameter was placed into the funnel and a 5 mm layer of vaseline oil was added to the glass bottle to minimize evaporation effects (IAEA, 1997). The precipitation and the streamflow water samples were collected in 2 ml amber glass containers, covered with parafilm, and stored unexposed to sunlight until laboratory analysis (Mook & Rozanski, 2000).

The stable isotopic composition of the collected water samples was measured using a cavity ring-down spectrometer L1102-I (Picarro, USA) with a precision of 0.1‰ for O^{18} . Samples of the same water type were analyzed consecutively to minimize the memory effect (Penna et al., 2010). Six sample injections were carried out to determine the isotopic composition of the samples. Following the manufacturer's recommendation to further diminish the memory effect, the measurements from the first three injections were discarded. Of the last three injections, the maximum difference of $\delta^{18}\text{O}$ was calculated and compared with the analytic precision of the equipment, as well as with the standard deviation of the isotopic composition of the standards used for analysis. Quality control of the results was carried out, and samples that presented measurement differences greater than those values were reanalyzed. Organic contamination of the isotopic signal was checked with the ChemCorrect 1.2.0 software (Picarro, 2010). In accordance with the Vienna Standard Mean Ocean Water, the results are provided in delta notation (δ) and expressed per mil (‰; Craig, 1960).

2.4. Mean transit time modelling

The MTT of streamflow was estimated using the lumped convolution approach (LCA), which assumes steady-state conditions in the hydrological system (Amin & Campana, 1996; Małoszewski & Zuber, 1982). To cope with this assumption, only water

samples collected during baseflow conditions were used for the analyses (i.e., samples collected during rainstorm events were discarded; McGuire, DeWalle, & Gburek, 2002). In recent years, alternative metrics have been developed to overcome the limitations of the steady-state assumption, as catchments do not always present stationary conditions (Kirchner, 2016a; Kirchner, 2016b). However, it has been demonstrated that the ZEO presents a high degree of homogeneity as a result of the low temporal variability of precipitation (Padrón et al., 2015), high atmospheric humidity throughout the year (approximately 94%; Córdova et al., 2015), compact geology, and relatively homogeneous distribution of the soils across the study catchments (Mosquera et al., 2015). Consequently, the steady-state assumption of the LCA is considered valid for the study area.

The LCA is based on the application of a predefined transit time distribution (TTD) that represents the transit times of all water molecules within the catchment storage. Mathematically can this be expressed by the convolution integral (Eq. 1), which transforms the input tracer signal (precipitation) into the output tracer signal (streamflow; Małoszewski & Zuber, 1982):

$$\delta out(t) = \int_0^{\infty} g(\tau) \delta in(t - \tau) d\tau \quad (Eq. 1)$$

where τ is the integration variable representing the MTT of the tracer through the system, t is the time of interest, which means the time of exit from the system, $\delta out(t)$ is the tracer composition at time t at the system's outlet, $g(\tau)$ is the TTD, and $\delta in(t - \tau)$ is the input tracer composition at the time $(t - \tau)$.

TTDs are theoretical transfer functions representing the flow system (Małoszewski & Zuber, 1982; McGuire & McDonnell, 2006). A previous MTT investigation at the study area presented a detailed assessment of 5 different TTDs and identified the exponential model (EM) as the one that best represents the hydrological behavior of the ZEO catchments (Lazo et al., 2019; Mosquera et al., 2016). The EM, which represents the hydrological system as a well-mixed reservoir (Eq. 2), was therefore used in this study.

$$g(\tau) = \frac{1}{\tau} \exp\left(\frac{-t}{\tau}\right) \quad (Eq. 2)$$

where τ is the MTT of water in the system, being the only parameter calibrated for the EM. Given the different time resolutions at which data were collected (sub-daily to monthly), the model was run at the coarser resolution (i.e., monthly). This decision was made to homogenize the dataset to avoid introducing uncertainties by filling data gaps during periods when only monthly data were available (i.e., 2016) and/or estimating and comparing the MTTs using data collected at different temporal frequencies (Stockinger et al., 2016; Timbe et al., 2015). To this end, precipitation isotopic data collected at finer temporal resolution were volume-weighted using their corresponding rainfall amounts to be converted into a monthly time series.

A significant proportion of runoff in most watersheds is generated by water that does not carry the signal of recent rainfall (Renshaw et al., 2003), thus the stream tracer response depends on the actual tracer mass flux. For this reason, a mass-weighted input function was used to take into account water recharge to the catchments (Mcguire & McDonnell, 2006):

$$\delta out(t) = \frac{\int_0^{\infty} g(\tau) \omega(t-\tau) \delta in(t-\tau) d\tau}{\int_0^{\infty} g(\tau) \omega(t-\tau) d\tau} \quad (Eq.3)$$

where $\omega(t)$ is a recharge mass variation function. The recharge function was estimated using the precipitation amounts corresponding to the monthly $\delta^{18}\text{O}$ composition of precipitation.

The MTT evaluation was conducted for the whole study period (May 2011-December 2018) and yearly periods using a monthly moving window at all catchments (M1-M8). The yearly time scale of analysis was chosen because MTTs at the ZEO are shorter than 1 year for all catchments (Mosquera et al., 2016). Thus, since the LCA assumes steady-state conditions, it is assumed that a 1-year period of analysis is enough to fulfill this assumption. Regarding the monthly moving window, the yearly MTTs were estimated for complete hydrologic years starting at different months. For example, if the first MTT was estimated for the period May 2011-April 2012, the following was estimated for the period June 2011-May 2012, and so on. This framework was adopted to investigate the temporal variability of MTTs for all catchments.

The Kling-Gupta Efficiency Coefficient (KGE) was used to assess the model's performance. The KGE is a goodness of fit metric between the observed and simulated streamflow isotopic composition (Gupta et al., 2009). This metric was chosen because within a single objective function, it takes into consideration correlation, variability, and bias error. The KGE coefficient ranges from $-\infty$ to 1, where negative values indicate a poor model performance, a value of zero indicates that the mean is a better representation of the system than the model, and a value of one indicates a perfect fit of the model to the observations. In the present study, models with KGE values higher than 0.45 were considered good predictions (Timbe et al., 2014). Initially, a Monte Carlo sampling procedure was employed to conduct 10.000 simulations using a τ parameter value randomly selected from a uniform distribution (Beven & Freer, 2001). Given that the stable isotopes of water permit estimating MTTs of water up to 5 years in age and the model was run at a monthly time scale, the range of τ values used for model calibration varied between 0 and 65 months (i.e., 0-5 years). Once the parameter value that yielded the highest KGE was identified, the model was run again using a narrowed parameter range until at least 1000 behavioral solutions, i.e., simulations with at least 95% of the highest KGE were obtained (Timbe et al., 2014). The Generalized Likelihood Uncertainty Estimation (GLUE) was used for quantifying the uncertainty of the model predictions (Beven & Binley, 1992) as the 5 and 95% limit bounds of the behavioral solutions (Timbe et al., 2014).

2.5. Evaluation of factors controlling the temporal variability of MTTs

The analysis of the hydrometeorological factors controlling the temporal variability of MTTs was conducted for all catchments (M1-M8). The following variables were used as potential predictors of the MTT temporal variability: precipitation amount (maximum, median, cumulative, and average), runoff coefficient, specific discharge (maximum, minimum, median, cumulative, and average), and non-exceedance streamflow rates (Q_{10} to Q_{90}). The following meteorological variables were also assessed: air temperature (maximum, minimum, median, and average), relative humidity (maximum, minimum, median, and average), solar radiation (maximum, minimum, median, and average), and evapotranspiration (maximum, minimum, median, cumulative and average). Given the small drainage area of the ZEO catchment ($<10 \text{ km}^2$), it was assumed that the spatial variation of evapotranspiration is the same for all the catchments (M1-M8). This is because the spatial distribution of vegetation and soils is similar throughout the catchment (Mosquera et al., 2016). Previous research at the study area showed that net radiation related to temperature is the major factor controlling evapotranspiration (Ochoa-Sánchez et al. 2020). In addition, the variation of air temperature decreases with altitude with an average thermal gradient of 0.5 to 0.7° C per 100 m (Van der Hammen & Hooghiemstra, 2000; Castaño, 2002). Therefore, the variation in evapotranspiration among the catchments is expected to be minimal since the altitudinal difference across the ZEO is small (3505 and 3900 m a.s.l., Mosquera et al., 2016).

Since the yearly-estimated MTTs can vary as a function of current and/or antecedent hydrometeorological conditions, the aforementioned variables were aggregated yearly not only for the same period in which the MTT estimation was conducted but also during antecedent periods corresponding to 1 to 12 months before the period in which the MTT estimation was conducted. For example, for the MTT estimated using the isotopic data for the period January 2017-December 2017, the hydrometeorological variables used for further evaluation were aggregated yearly for the following periods: the same period for which the MTT was estimated, the period October 2016-September 2017 (i.e., 3 months before the MTT estimation period), July 2016-June 2017 (i.e., 6 months before the MTT estimation period), and so on up to 12 months before the MTT estimation period. These hydrometeorological variables were also aggregated for periods that included the same period used for the estimation of the MTT plus 3, 6, 9, and 12 months back (0+15, 0+18, 0+21, and 0+24 months, respectively). For example, for the MTT estimated using the isotopic data for the period January 2017-December 2017, the hydrometeorological variables were aggregated for the following periods: the period October 2016-December 2017 (i.e., 15 months since the beginning date of the MTT modelling or 0+15 months), the period July 2016-December 2017 (i.e., 18 months since the beginning date of the MTT modelling or 0+18 months), and so on until 24 months since the beginning date of the MTT modelling (0+24 months). Assuming steady-state conditions, and since MTTs at the ZEO during the period 2011-2014 were shorter than 1 year (Mosquera et al., 2016), aggregation of the hydrometeorological variables up to 1-year before the period in which MTTs were estimated were considered as the antecedent periods that could influence the MTTs of the catchments.

The aforementioned hydrometeorological variables were used as potential factors controlling the temporal variability of MTTs. As a first step, the Pearson correlation analysis (r) was conducted. The T-test at a 95% confidence level ($p<0.05$) was used to assess the statistical significance of the correlations. After performing the correlations, more than one predictor variable was found to be acceptably correlated ($r>0.5$) with the MTTs (further information provided in Supplementary material S1). In a second step, a multicollinearity analysis was carried out to prevent that two or more highly correlated explanatory variables might provoke unreliable predictions (Yu, Jiang, & Land, 2015). A correlation matrix among the independent variables was used to exclude redundant variables. For this purpose, a threshold of coefficient of determination (R^2) greater than 0.75 was applied (Siegel, 2016). Then the variance inflation factor (VIF) criteria equal to or less than 3 were applied to the remaining variables. This analysis allowed avoiding overfitting issues, which could potentially obscure important relations among variables (Lin, Foster, & Ungar, 2011). Following the multicollinearity analysis, the multiple linear regression (MLR) was carried out through a forward criterion using the root mean square error (RMSE) as objective function (Montgomery, Jennings, & Kulahci, 2015). The forward criterion starts without any predictor variables, and then adds additional variables one by one as the RMSE decreases (Derksen & Keselman, 1992). The MLR was implemented on R studio software version 4.0.2 using the *Caret* library. To assess the robustness of the MLR results, the leave-one-out cross-validation was applied (LOOCV; Efron & Gong, 1983; Stone, 1974). Given 57 MTT estimations were available for each study catchment for all antecedent conditions, MLR models up to 5 variables were considered since a threshold of one variable per ~10 observations is recommended (Austin & Steyerberg, 2015; Vittinghoff & McCulloch, 2007).

The performance of the models was evaluated using R^2 and adjusted R^2 (R^2_{adj}), the Akaike Information Criterion (AIC), p-values of the F-test and the mean absolute error (MAE). R^2 assumes that every explanatory variable in the model helps explain the variance in the dependent variable, whereas R^2_{adj} gives the percentage of variation explained by only those explanatory variables that affect the dependent variable and penalizes the addition of independent variables (Pham, 2019). As a criterion of information of the parsimony, the Akaike Information Criterion (AIC) was selected with the smallest values (Akaike, 1974). The F-test at a 95% confidence level ($p<0.05$) was used to assess the statistical significance of the regressions. After 5 models were tested, the model which accomplishes the following two criteria was chosen: adjusted R^2 greater than 0.5, and MAE around half the standard MTT variation (approximately less than 20% of the MTT variability; Santhi et al., 2001).

3. Results

3.1. Hydrometeorological and isotopic characterization

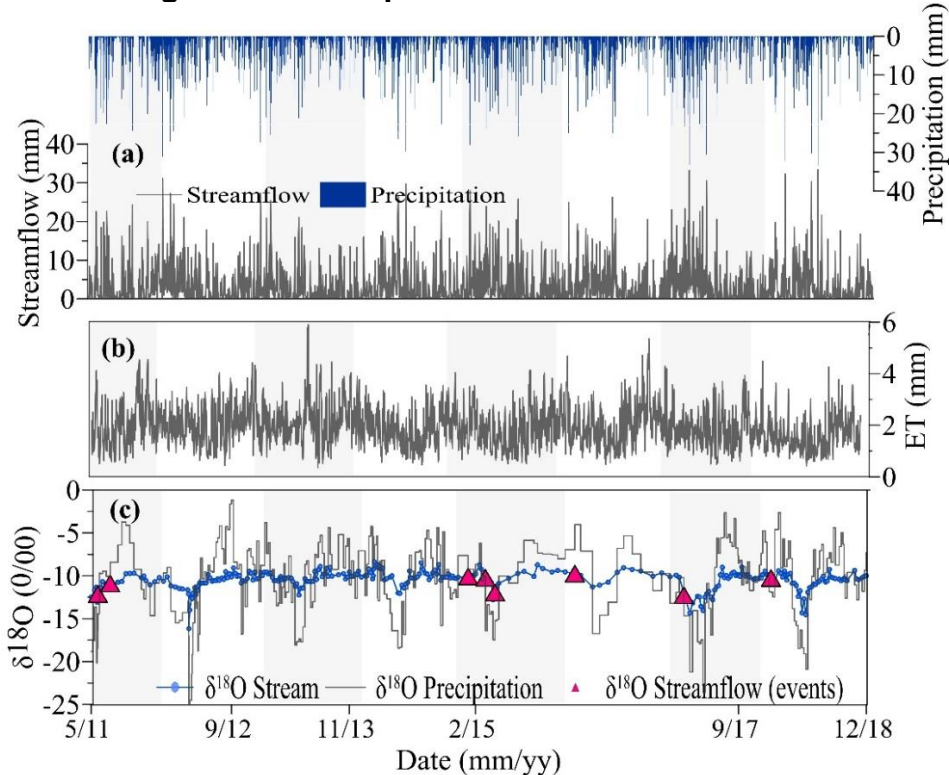


Figure 2. Time series of hydrometeorological and stable isotopic data in the period May 2011 - December 2018. **(a)** Daily precipitation and streamflow; **(b)** daily evapotranspiration, and **(c)** $\delta^{18}\text{O}$ isotopic composition of precipitation and streamflow of catchment M6 collected at event-based (sub-daily) and monthly frequency (the triangles show the $\delta^{18}\text{O}$ isotopic data collected during rainfall events). The white/light gray shaded areas indicate yearly periods.

Catchment M6 is representative of the hydrological behavior of the ZEO (Lazo et al., 2019) and tropical alpine (Páramo) catchments in Southern Ecuador (Ramón et al., 2021). Figures 2a and 2b show the hydrometeorological conditions of the ZEO during the period May 2011-December 2018. Precipitation was fairly evenly distributed throughout the year and streamflow response to precipitation inputs was flashy during study period (Fig. 2a). Mean annual precipitation (\pm standard deviation) for the entire period was 1222 ± 22 mm and ranged from 1335 to 1035 mm. The driest years were 2013 (1035 mm) and 2014 (1175 mm), while the wettest years were 2011 (1335 mm) and 2012 (1312 mm). Precipitation during the wettest months varied from 161 mm (February 2011 and May 2014) to 236 mm (March 2017), while during the driest months precipitation ranged from 24 mm (August 2016) to 51 mm (February 2014). Annual average streamflow (Fig. 2b) was 648 ± 42 mm and varied from 548 mm (2018) to 780 mm (2011). The temporal variation of reference evapotranspiration (ET) for the study period is shown in Fig. 2b.

Mean annual ET was 694 ± 64 mm, ranging between 791 mm (2013) and 589 mm (2018). The mean $\delta^{18}\text{O}$ isotopic composition of precipitation during the study period was $-10.3 \pm 3.6\text{ ‰}$ (max: -1.2 ‰ ; min: -24.9 ‰). It showed a large temporal variability, with isotopically depleted values during the wettest periods (March-May), and enriched values during the less wet ones (August-October; Fig. 2c). The $\delta^{18}\text{O}$ isotopic composition in streamflow was more attenuated ($-10.7 \pm 0.1\text{ ‰}$; Table 1) than $\delta^{18}\text{O}$ in precipitation. The isotopic variability of stream water was similar at all catchments, except for M7 whose isotopic composition strongly resembled that of precipitation given that it works as a shallow ponded wetland in which precipitation water leaves the catchment rapidly (Correa et al., 2018; Lazo et al., 2019; Mosquera et al., 2016).

Table 1. Summary statistics of the $\delta^{18}\text{O}$ isotopic composition in precipitation (P1) and streamflow (M1-M8) collected during the period May 2011 - May 2018.

Sampling Station	Altitude (m.a.s.l)	# samples	$\delta^{18}\text{O}$ Streamflow (‰)			
			Average	SE	Max	Min
M1	3840	349	-10.7	0.06	-6.8	-18.0
M2	3840	359	-10.5	0.06	-7.2	-15.4
M3	3800	329	-10.8	0.05	-8.7	-16.3
M4	3800	382	-10.6	0.06	-8.1	-16.5
M5	3800	307	-10.7	0.06	-8.6	-16.4
M6	3780	293	-10.5	0.07	-8.4	-16.2
M7	3820	286	-9.5	0.14	-5.4	-16.6
M8	3700	404	-9.9	0.06	-7.5	-14.3
P1	3779	310	-10.3	0.24	-1.2	-24.9

Abbreviation: **SE** standard error.

A total of 425 hydrometeorological variables were used to evaluate potential associations with the estimated MTTs for each catchment. Figure 3 shows the box plot of the hydrometric variables which were aggregated using the same time step as the MTTs for each of the studied catchments. Average streamflow (Q_{mn}) was 1.87 ± 0.30 and varied between 2.13 ± 0.25 and 1.61 ± 0.28 (Fig. 3a). Median streamflow (Q_{md}) was on average 1.08 ± 0.26 , varying from 1.25 ± 0.23 to 0.81 ± 0.22 , respectively (Fig. 3b). Average maximum streamflow (Q_{mx}) was 18.65 ± 3.19 and ranged from 21.29 ± 3.41 to 15.59 ± 2.69 (Fig. 3c). Average minimum streamflow (Q_{min}) was 0.12 ± 0.07 and varied from 0.05 ± 0.02 up to 0.30 ± 0.13 (Fig. 3d). Catchments M3, M4, and M5 had the highest Q_{min} compared to the others. In catchment M4, Q_{min} increased by 50%, higher compared to catchments M3 and M5. Q_{min} variation was similar in catchments M1, M6, M7, and M8. Low flows ($Q_{10}-Q_{30}$) in catchments M3, M4 and M5 were higher than in the rest of the catchments (Fig. 3e-3g). Intermediate streamflow rates ($Q_{40}-Q_{60}$) varied from 0.70 ± 0.06 to 1.22 ± 0.13 . For catchments, M1-M5 intermediate streamflow was approximately 50% higher than in the other catchments (Fig. 3h-j). High streamflow rates ($Q_{70}-Q_{90}$) were similar for all the catchments (Fig. 3k-3m). Their average values were 1.68 ± 0.18 , 2.77 ± 0.26 , and 4.04 ± 0.41 , respectively. Mean (P_{mn}) and median (P_{md}) precipitation were similar in all catchments, except in M7, where precipitation was 11% lower compared to the catchment

average (Fig. 3n-3o). The mean runoff coefficients (RC) of the catchments were 0.56 ± 0.06 and varied between 0.50 and 0.64, with the highest at catchment M5 and the lowest at catchment M8 (Fig. 3p).

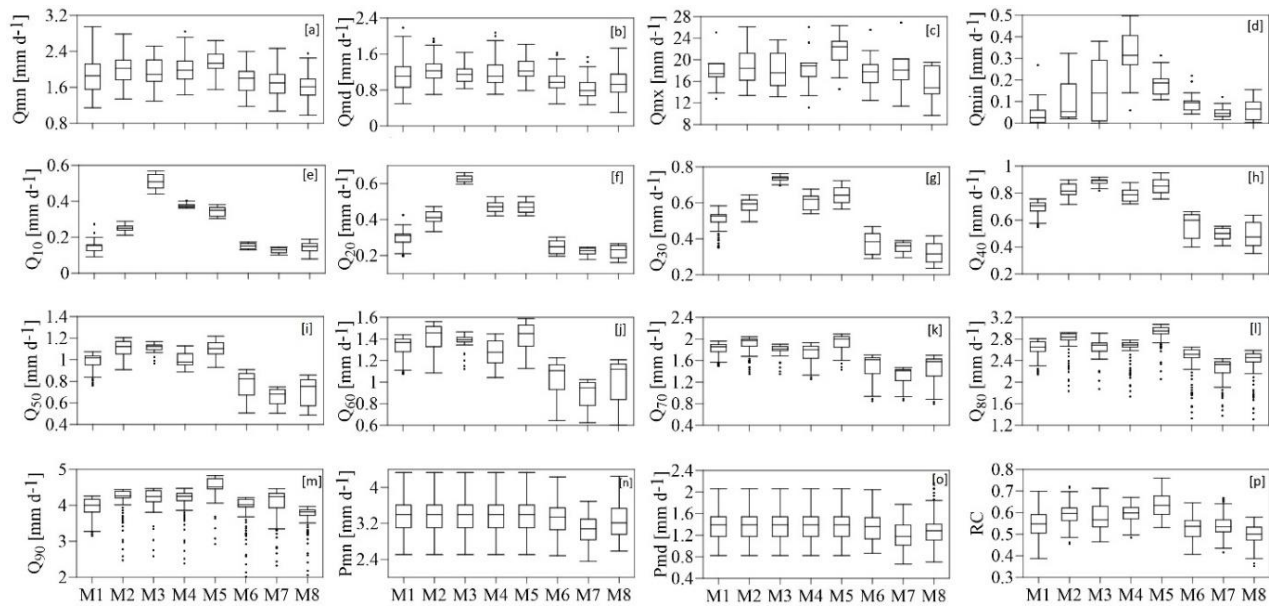


Figure 3. Box plots of the hydrometric variables for each of the studied micro-catchments (M1-M8) during the period May 2011 - December 2018 using a monthly moving window. The box represents the median and the interquartile range, the whiskers represent 1.5 times the interquartile range, and the black dots represent the outliers. Abbreviations: **Qmn** mean streamflow; **Qmd** median streamflow; **Qmx** maximum streamflow; **Qmin** minimum streamflow; **Q₁₀**, **Q₂₀**, **Q₃₀**..., **Q₉₀** streamflow rates as the frequency of non-exceedance; **Pmn** mean precipitation; **Pmd** median precipitation; **RC** runoff coefficient.

3.2. Mean transit time modelling

Results of the MTT analysis for representative catchments using the whole dataset (i.e., May 2011-December 2018) are shown in Fig. 4. Catchments M3 (Fig. 4a), M4, and M5 had the longest MTT varying between 8.6 months (258.6 days) and 10.8 months (324.4 days). Intermediate MTT values were identified for catchments M1, M2, M6 (Fig. 4b), and M8, varying between 5.3 months (158.9 days) and 8.1 months (244.2 days). Catchment M7 presented the shortest MTT (1.6 months or 49.1 days; Fig. 4c). All estimated MTTs were shorter than 1 year, and in all cases, the goodness of fit of the objective function was higher than the threshold for model acceptance (i.e., $KGE > 0.45$; Fig. 4).

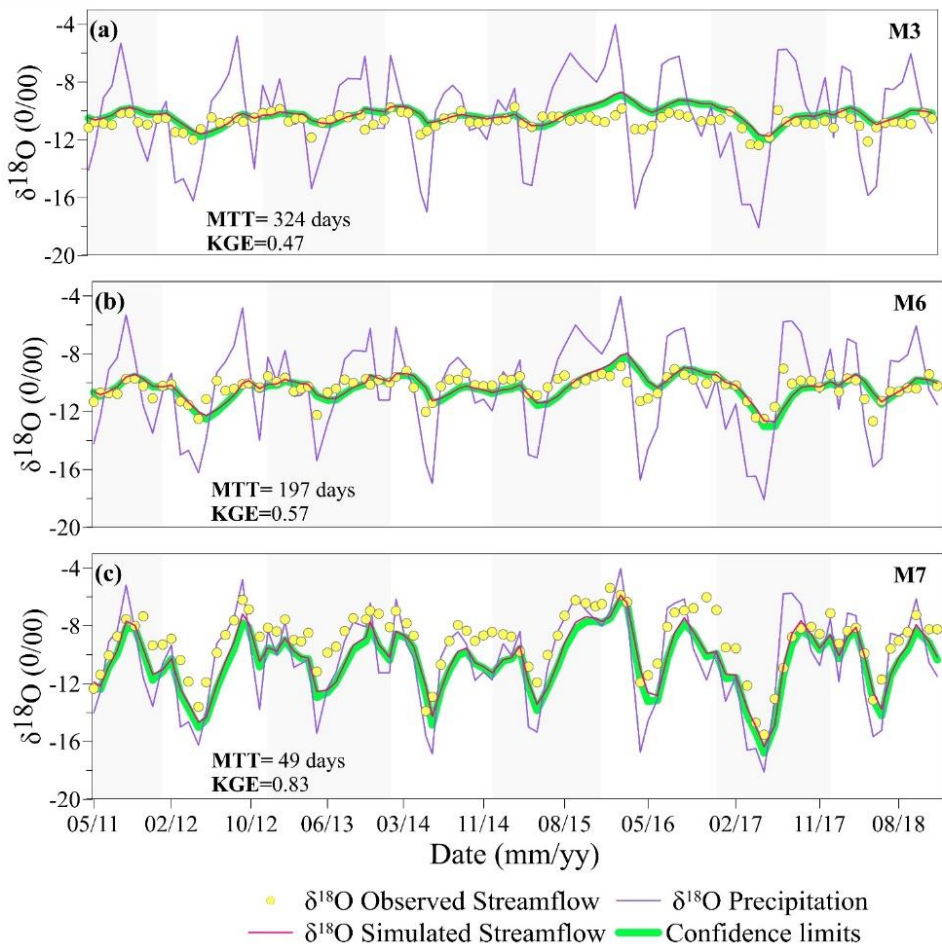


Figure 4. Observed and simulated $\delta^{18}\text{O}$ streamflow isotopic composition during the period May 2011 - December 2018 for catchments: (a) M3, (b) M6, and (c) M7. The green shaded area represents the 5-95% confidence limits based on the MTT parameter values used in the simulations. The white/light gray shaded areas indicate yearly periods.

Analysis of the MTTs estimated for yearly periods using a monthly moving window resulted in 81 fit models per study catchment. Results of this analysis for catchment M6 are shown in Fig. 5. For this catchment, the average (\pm standard deviation) value of the MTTs were 5.9 ± 1.4 months (175.5 ± 41.7 days). KGE values of the associated simulations were higher than the threshold for model acceptance, ranging between 0.45 and 0.77 (Fig.5). MTTs ≥ 4 months and < 8 months accounted for 87.6%, 7.4% of them were higher than 8 months, and the remaining 5% were shorter than 4 months. The longest MTTs were observed from late-2014 to mid-2015, while the shortest occurred in early-2014 and from mid-2017 to the end of the study period (December 2018; Fig. 5). A similar temporal variability of MTTs was observed for the rest of the ZEO catchments using a monthly moving-window approach.

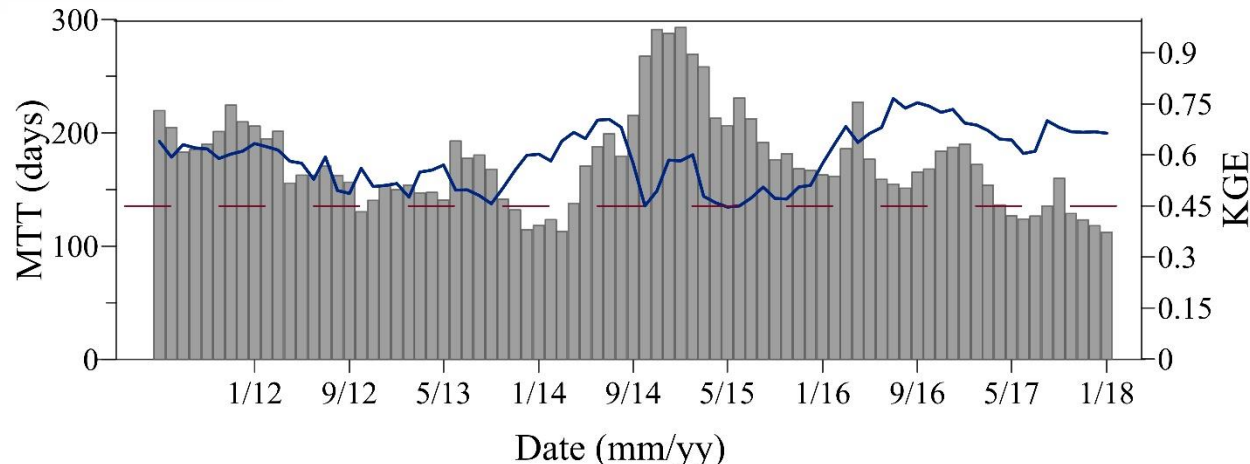


Figure 5. Yearly estimated MTTs using a monthly moving window for catchment M6 (gray bars) during the period May 2011 - December 2018. The MTTs correspond to the parameter value that yielded the highest KGE value during the simulations (blue line). The dashed red line represents the KGE value of 0.45 considered in this study as a threshold between good (values above) and poor (values below) model predictions. The figure only shows the beginning date of each yearly moving window (i.e., the MTT and KGE values corresponding to August 2014 were obtained for the simulation period August 2014 - July 2015).

Yearly estimated MTTs for all study catchments indicated the dominance of short MTTs (i.e., 96% of them were shorter than 1 year) across the ZEO (Fig. 6a), associated to generally acceptable KGE values that varied between 0.51 ± 0.15 and 0.82 ± 0.05 (Fig. 6b). Similar to the results using the complete dataset, catchments M3 (9.3 ± 2.3 or 278.1 ± 68.3 days), M4 (7.9 ± 2.1 months or 236.6 ± 63.1 days), and M5 (8.0 ± 1.9 months or 239.9 ± 56.0 days) presented the longest MTTs (Fig. 6a). Catchments M1 (7.1 ± 2.1 months or 213.2 ± 63.8 days), M2 (5.3 ± 1.1 months or 159.1 ± 33.9 days), M6 (5.9 ± 1.4 months or 175.5 ± 41.7 days), and M8 (5.8 ± 1.3 months or 175.3 ± 37.5 days) showed intermediate MTT values. The shortest MTTs were found at M7 (1.8 ± 0.4 months or 52.4 ± 12.1 days).

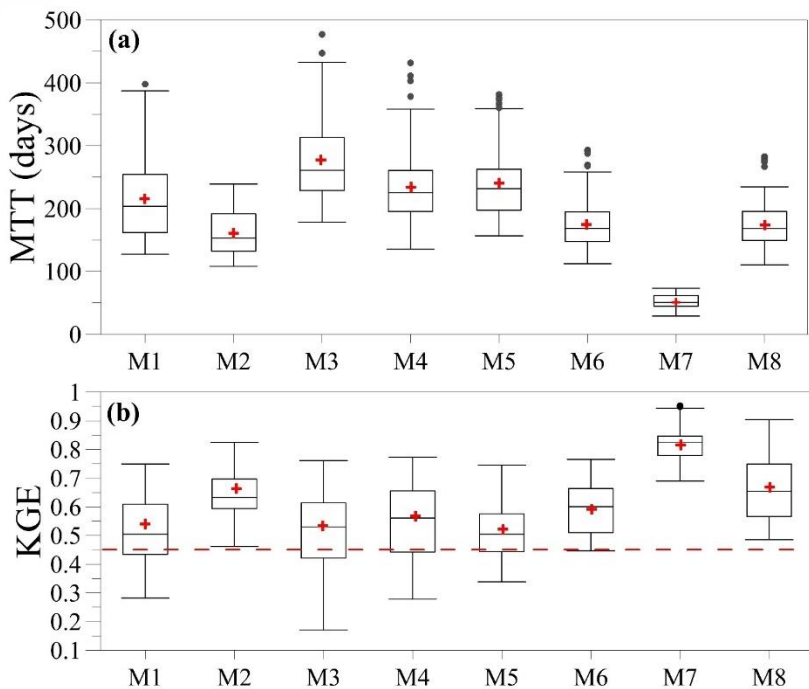


Figure 6. Box plots of the (a) yearly estimated MTTs using a monthly moving window for catchments M1-M8, and (b) their corresponding KGE values. The box represents the median and interquartile range, the whiskers represent 1.5 times the interquartile range, and the black dots represent the outliers. The red crosses represent the average of the distributions of MTT and KGE values. The dashed red line in subplot (b) represents the KGE value of 0.45 considered in this study as a threshold between good (values above) and poor (values below) model predictions.

3.3. Identification of factors controlling the temporal variability of MTTs

Linear correlation results showed that several hydrometeorological variables were at least acceptably correlated ($r>0.5$) with the yearly estimated MTTs for all analyzed catchments (Supplementary material S1; Fig S1). The subsequent VIF multicollinearity analysis allowed identifying between 8 and 11 independent variables which could significantly explain the MTT temporal variability of the catchments (more details in Supplementary material S2). Those variables were used to identify the main hydrometeorological factors controlling the temporal variability of baseflow MTTs through MLR analysis. Since the presented analysis was carried out at a monthly time scale, analysis for catchment M7 – which presented very short water ages (1-2 months) – could not be pursued as its MTT temporal variability is likely dependent on antecedent conditions on the order of days or weeks. For the rest of the catchments, Table 2 shows the results of the MLR models accomplishing the conditions for best model selection. That is, the MLR model with the least number of predictive variables fulfilling both criteria for best model selection in terms of error reduction ($\text{RMSE}\sim 0$) and goodness of fit ($R^2_{\text{adj}}>0.5$).

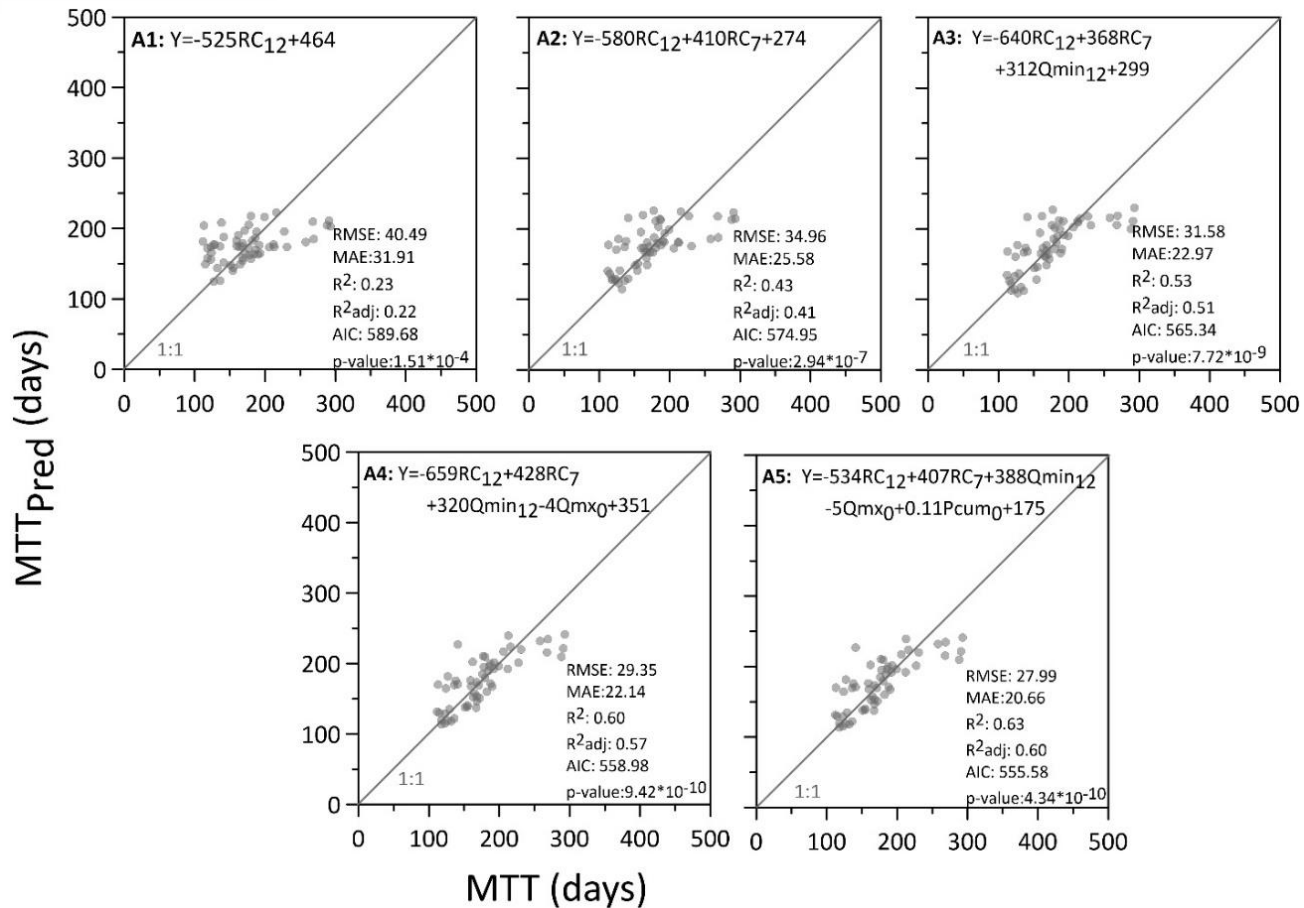


Figure 7. Multiple linear regression models for micro catchment M6 for the period May 2011 - December 2018 using hydrological and meteorological variables as predictors. **A1** to **A5** represents different models after incorporation of the explanatory variables. The number next to the hydrological variable indicates the corresponding moving window. Abbreviations: **RC** runoff coefficient; **Qmin** minimum streamflow; **Qmx** maximum streamflow; **Pcum** cumulative precipitation. The dashed line shows the 1:1 ratio relation.

Results of the MLR analysis for catchment M6 are shown in Fig. 7. Eight hydrometeorological variables were considered in the MLR models of this catchment after performing the collinearity analysis: ET_{min6} , Q_{max0} , P_{cum0} , RC_7 , Q_{min12} , RC_{12} , P_{cum15} , and RC_{18} . MLR models up to 5 variables were evaluated using these variables (models A1 to A5). Results of the 5 MLR models (A1 to A5) are described below. Model A1 included RC_{12} as the only predictive variable and explained 22% of the dataset variance. Model A2 included two variables, namely RC_7 and RC_{12} , and allowed explaining 41% of the dataset variability. Model A3 included 3 variables, Q_{min12} , RC_7 , and RC_{12} , explaining 51% of the variance. Model A4 included all variables in model A3 and Q_{max0} , explaining 57% of the MTTs temporal variation. Model A5 included all variables in model A4 and P_{cum0} (5 variables in total) and accounted for 60% of the dataset variability. The difference in RMSE between the models decreased from 5.53 for model A1 to 1.36 for

model A5. Model A3 was selected as the one best resembling the temporal variability of MTTs for catchment M6 as it complied with the aforementioned conditions for model acceptance.

The same analysis conducted for the remaining catchments indicated that the number of variables necessary to achieve model acceptance conditions for each of them varied between 2 and 5 (Table 2). Two predictive variables were used for catchments M1 (Q_{md8} and $Q_{min0+15}$), M2 (Q_{min10} and P_{cum0}), and M3 ($Q_{300+18}+Q_{md7}$). The MLR for catchment M4 required 3 predictive variables (Q_{300+18} , RC_9 , and Q_{mx7}). The models for catchments M5 and M8 required the largest number of predictive variable, 4 for the former (Q_{md12} , Q_{cum24} , P_{mx12} , and Q_{cum9}) and 5 for the latter (Q_{min12} , P_{md10} , P_{mx9} , Q_{mx12} , and Q_{cum0}). All of these models presented relatively low RMSE (from 22.60 to 47.98). The models had R^2_{adj} values ranging from 0.50 and 0.58 (Table 2), indicating that all models explain at least 50% of the MTT temporal variability for each catchment. The average AIC value among catchments was low (581 ± 87), suggesting that the selected models are parsimonious. Results from the F-tests show that all models are significant at $p<10^{-9}$. This means there is evidence of the existence of linear relationship between MTTs and hydrometeorological variables.

Table 2. Factors controlling the temporal variation of MTTs using multiple linear regression (MLR) with their respective statistical metrics for catchments M1-M8 during the period May 2011 - December 2018.

Catchments	Variables used in the MLR models	n	m	RMSE	MAE	R ²	R ² _{adj}	AIC	p-value
M1	Qmd ₈ +Qmin ₀₊₁₅		8	42.29	32.50	0.59	0.58	596.64	2.53*10 ⁻¹¹
M2	Qmin ₁₀ +Pcum ₀		10	22.60	17.00	0.52	0.50	525.21	2.74*10 ⁻⁰⁹
M3	Q30 ₀₊₁₈ +Qmd ₇		8	47.98	35.03	0.59	0.57	611.03	4.15*10 ⁻¹¹
M4	Q30 ₀₊₁₈ +RC ₉ +Qmx ₇	57	9	47.63	35.41	0.55	0.52	612.20	2.80*10 ⁻⁰⁹
M5	Qmd ₁₂ +Qcum ₀₊₂₄ +Pmx ₁₂ +Qcum ₉		9	41.03	32.87	0.56	0.53	597.19	7.97*10 ⁻⁰⁹
M6	RC ₁₂ +RC ₇ +Qmin ₁₂		8	31.58	22.97	0.53	0.51	565.34	7.72*10 ⁻⁰⁹
M8	Qmin ₁₂ +Pmd ₁₀ +Pmx ₉ +Qmx ₁₂ +Qcum ₀		11	28.46	22.41	0.54	0.50	557.47	9.01*10 ⁻⁰⁸

Abbreviations: **Qmd** median streamflow; **Qmin** minimum streamflow; **Qcum** accumulated streamflow; **RC** runoff coefficient; **Pcum** accumulated precipitation; **Pmd** median precipitation; **n** number of samples used for the multiple linear regressions; **m** the number of variables used for the Multiple Linear Regressions; **RMSE** root mean square error; **MAE** mean absolute error; **AIC** Akaike information criterion (Akaike, 1974). The number next to the hydrological variable indicates the corresponding moving window. * Catchment M7 did not take it into account because the MTTs are less than 1 month and the moving window used was for 1 month back, so this catchment did not yield good results.

4. Discussion

4.1. Mean Transit Time Modelling

Taking advantage of an 8-year data set from a nested system of tropical Andean catchments, this study addresses one of the 23 unsolved problems in hydrology (Blöschl et al., 2019): how old is stream water and how water ages vary in time. To this end, it is necessary to evaluate the assumptions of the applied MTT modelling approach. One limitation of the LCA for estimating MTTs is the fulfillment of the assumptions of hydrological stationarity (i.e., invariance in time) and homogeneity of the studied catchments (J. Kirchner, 2016). Despite the variety of hydrometeorological conditions occurring at the ZEO during the 8-years study period, the temporal variability of MTTs across the catchments was small (191.30 ± 47.10 days). Contrary to evidence of non-stationary conditions in other tropical (Birkel et al., 2016) and non-tropical montane catchments (Peralta-Tapia et al., 2016), this observation supports the hypothesis that the ZEO catchments function under stationary conditions. This, as a result of homogeneous landscape characteristics (i.e., vegetation and soil distribution, topography, and geology) and low temporal variability of climate conditions (Correa et al., 2017; Lazo et al., 2019; Mosquera et al., 2016). This finding also suggests that the ZEO catchments meet the steady-state assumptions of the LCA applied to estimate the presented MTTs. In addition, the fact that the estimated MTTs were shorter than the yearly periods applied to investigate MTT temporal variability in this study indicates that our results can be considered reliable and robust as evidenced by the low uncertainty in the modelling results.

These considerations are important to note since a previous evaluation of MTT temporal variability in a tropical setting yielded results with high uncertainty (Birkel et al., 2016). This, most likely related to an incorrect application of the LCA as MTTs were calculated for periods shorter than a hydrological year (i.e., 4-months) in a highly seasonal montane catchment in Costa Rica, which violates the steady-state assumptions of the LCA. Furthermore, the estimated MTTs were often larger than the period of analysis, MTTs up to 1-year were reported, further emphasizing the need to carefully consider the assumptions of the methodology used to obtain reliable MTT estimations.

The MTTs at ZEO were shorter than 1-year when modelled using both the complete dataset and yearly periods using a monthly moving window. These MTTs are consistent with typical values in pristine catchments of less than 10 km^2 in other regions (Tetzlaff et al., 2011; Hrachowitz et al., 2010; Soulsby et al., 2009). These values are also similar to prior MTT estimations in the same study area during the period 2011-2014 (up to 9 months; Mosquera et al., 2016). These findings support the idea of a rapid rainfall-runoff dynamics and a minimum contribution of groundwater to streamflow (Stewart et al., 2010; DeWalle et al., 1997). A rapid hydrologic response could be explained by the limited development of the soils (up to 1 m deep), presenting a porous and open soil structure with a high water storage capacity, particularly the riparian wetlands (Lazo et al., 2019).

Also, wetlands are hydrologically connected to slopes, especially during wet periods, and surface water does not evaporate strongly as humidity remains high throughout the year (>90%; Córdova et al., 2015). The short MTTs are likely influenced by the increasing humidity and the increased connectivity of shallow subsurface flow paths (Segura et al., 2012; Birkel et al, 2012a; Rinaldo et al, 2011). As a consequence, the soils remain wet most of the time, and their high porosity results in a fast mobilization of water throughout the entire soil profile (Mosquera et al., 2020), allowing for a continuous recharge of riparian wetlands which sustain flow production year-round (Mosquera et al., 2015).

In another study conducted in the Scottish Highlands, MTT temporal variability was assessed in two small catchments with different features (Hrachowitz et al., 2009). One of the catchments was characterized by low permeable gleyed soils overlying compacted geology. The second catchment was dominated by free-draining podzolic soils situated on deep extensively fractured bedrock. The former presented MTTs shorter than 1-year (135-202 days), agreeing well with our results as it presented similar conditions than the ZEO, and thus a comparable hydrological behavior in which soils remaining close to saturation favor a rapid response of streamflow via shallow subsurface with minimal contributions of groundwater. The latter had much longer MTTs (1830-1970 days) as a result of the dominance of a well-mixed groundwater reservoir in the system of bedrock fractures, differently from the ZEO. In other environments (i.e., temperate or boreal) MTTs show a large variability because groundwater influences them opposite to ZEO where MTTs vary little. In a study conducted in a temperate zone, MTTs were estimated using a 1-month moving window with a 10-year data set in five Japanese meso-catchments (Ma & Yamanaka, 2013, 2016). The average MTT across the catchments was 23.7 years, and the temporal variation was similar in the five sub-catchments ranging from 1.2 to 37 years. Contrary to our hydrological system, MTTs up to few decades reflect a delayed groundwater response and high water storage in the large groundwater reservoir of the Japanese catchments. In another study of a boreal catchment in Sweden MTTs ranged from 300 to 1400 days using a 10-year data set and a monthly moving window (Peralta-Tapia et al., 2016). These results differed from our study area because of the older groundwater contributions to streamflow and the large temporal changes in stored water due to strong climate seasonality across the year, unlike in our study where the water storage is continuously high due to sustained rainfall inputs throughout the year.

4.2. Identification of factors controlling temporal variability of MTTs

The main factors controlling MTT temporal variability at the ZEO are precipitation, streamflow, and runoff coefficient. It is reasonable that precipitation is a driver of MTTs as it acts as a “force” that pushes water out of the soil matrix, whereas streamflow reflects the system’s response to water mobilization (i.e., mixture of precipitation and soil water). At the ZEO, the rapid filling of the soil water reservoir during rainfall events (Correa, Ochoa-Tocachi, & Birkel, 2019) and the soil’s high-water storage capacity (Lazo et al., 2019) result in a soil system being moist year-round. This hydrological dynamic helps supply baseflow to streams and support the shallow water table of the paramo areas around the south Ecuadorian highlands. As a consequence, the amount of water available to move through the ZEO is a representation of rapid subsurface flow in the shallow layer

of the soils which remains near saturation, explaining runoff coefficient as a key variable influencing baseflow MTTs. For these reasons, it is not surprising that antecedent conditions of these hydrological variables up to 1-year influence MTT temporal variability, with the longest antecedent conditions found for spring-dominated catchments because of their higher water storage capacity (Lazo et al., 2019).

Similar results to our research were obtained in a boreal catchment in northern Sweden. In that catchment a strong correlation between annually estimated MTTs and yearly precipitation was found (Peralta-Tapia et al., 2016). The result obtained for this boreal catchment suggests MTTs are strongly influenced by precipitation. Precipitation variability had a marked influence on the resulting MTT estimates as it affects antecedent soil moisture conditions. In our study area, the longest MTTs occurred during the less wet periods (a period conditioned by lower input precipitation than average) and the shortest ones during the wettest ones in which rapid runoff was facilitated by soil rich in organic matter, high saturated hydraulic conductivity, and compacted underlying geologic layers. MTT variability was also found to be controlled by the amount of precipitation in two Zero-Order catchments in the USA (Heidbüchel, Troch, & Lyon, 2013). Similar to our findings, these authors reported that precipitation events during the wettest periods caused the water storage capacity of soils to reach saturation, resulting in fast runoff composed of younger water.

In contrast to our findings, the amount of stored groundwater was found as a primary control on MTTs temporal variation in a temperate meso-catchment in Japan (Ma & Yamanaka, 2016). These results differ from ours because deep groundwater contributions at the ZEO are almost negligible. Similar to our findings, MTTs were also found to be correlated with runoff coefficient in a semi-arid catchment in southeastern Australia (Cartwright & Morgenstern, 2015; Cartwright et al., 2020). Nevertheless, different processes explain the identified relations in the Australian study site and ours. High evaporation and transpiration rates, low precipitation inputs, and hence a reduced rate of groundwater recharge help explain the temporal variability of MTTs in the semi-arid environment. Differently, fairly sustained precipitation inputs (Padron et al., 2016) and low transpiration rates (Ochoa-Sánchez et al., 2020) in combination with almost negligible contributions of deep groundwater (Mosquera et al., 2020; Mosquera et al., 2016) likely explain the relation between MTTs and runoff coefficient at the ZEO catchments.

The fact that evapotranspiration was not found as a factor controlling MTT temporal variability suggests that local climate has little to no influence on how water mixes in the subsurface. The latter most likely because of the high air humidity and limited available energy at ZEO year-round (Córdova et al., 2016; Ochoa-Sánchez et al., 2020). This finding is in line with a previous investigation in 20 Scottish highland catchments with similar landscape and climate conditions than at our study site (Hrachowitz et al., 2009).

However, this finding contrasts with a previous investigation in a tropical catchment in Costa Rica in which wind speed was found to be strongly correlated with MTTs (Birkel et al., 2016). The authors attributed this observation to a relation between the origin of air

masses contributing to local precipitation, which in turns could influence the water storage of the catchment. Nevertheless, these findings are potentially biased given that the study was conducted using a short time series of isotopic data (2-years) and the aforementioned non-compliance with the assumptions of the LCA. The former relates to the lack of a sufficiently long period of analysis to cover a wide range of hydrometeorological conditions, and the latter to the large uncertainties in the MTT calculations. Both of these factors raise some questions about the validity of the results, as they could have produced spurious correlations with meteorological variables. On the contrary, the fact that we used a dataset covering several hydrometeorological cycles and the identified variables influencing streamflow MTT variability comply reasonably with the conceptual model of the catchments further supports the robustness of our results and the validity of our findings for improved decision making.

Although there are similarities and differences among the findings of previous studies and ours, there are no investigations reporting the combination of streamflow, precipitation, and runoff coefficient to identify the factors controlling the temporal variability of MTTs in the tropics and elsewhere. This may result from the strong interplay between precipitation and streamflow dynamics, which controls subsurface water transport and mixing processes in our study area under the presence of riparian wetlands connected to the stream network and the virtually absent contribution of deep groundwater storages (Mosquera et al., 2015).

5. Conclusion

This study contributes to improved understanding of the underlying causes of MTT temporal variability in montane catchments in remote regions. According to the obtained results it can be concluded that:

- MTTs in tropical alpine catchments are shorter than 1-year and present a small temporal variation, indicating the prevalence of steady-state conditions and that lumped models represent a useful tool to investigate hydrological dynamics in the region.
- The factors that control the temporal variability of MTT across the catchments were precipitation, streamflow, and runoff coefficient under different antecedent conditions up to 1-year, supporting previous conceptualizations of runoff generation in the study area that suggested a hydrological system dominated by the connectivity of subsurface flow paths through shallow organic soil layers.

These results highlight the importance of testing the temporal variation of the MTTs before their application in strategies and planning-decisions in water management and climate adaptation measures. If moisture conditions change, shorter MTTs can impact nutrient removal and pollutant export. Changes in climate or land-use could also cause variations in the ages of stream water, and should be assessed in future investigations. Further research involving the factors controlling MTTs at larger spatial scale for tropical alpine catchments is also recommended. Also, it would be interesting to assess the influence of fog in the temporal variability of MTTs since this hydrological process has been observed to increase precipitation up to 20% in the study area.

6. References

Akaike, H. (1974). A New Look at the Statistical Model Identification. *IEEE Transactions on Automatic Control*, 19(6), 716–723. <https://doi.org/10.1109/TAC.1974.1100705>

Allen, R., Pereira, L., Raes, D., Smith, M. (1998). Crop evapotranspiration-Guidelines for computing crop water requirements-FAO Irrigation and drainage paper 56. *FAO, Rome*.

Amin, I. E., & Campana, M. E. (1996). A general lumped parameter model for the interpretation of tracer data and transit time calculation in hydrologic systems. *Journal of Hydrology*, 179(1–4), 1–21. [https://doi.org/10.1016/0022-1694\(95\)02880-3](https://doi.org/10.1016/0022-1694(95)02880-3)

Austin, P. C., & Steyerberg, E. W. (2015). The number of subjects per variable required in linear regression analyses. *Journal of Clinical Epidemiology*, 68(6), 627–636. <https://doi.org/10.1016/j.jclinepi.2014.12.014>

Benettin, P., Rinaldo, A., & Botter, G. (2015). Tracking residence times in hydrological systems: Forward and backward formulations. *Hydrological Processes*, 29(25), 5203–5213. <https://doi.org/10.1002/hyp.10513>

Beven, K., & Binley, A. (1992). The future of distributed models: Model calibration and uncertainty prediction. *Hydrological Processes*, 6(3), 279–298. <https://doi.org/10.1002/hyp.3360060305>

Beven, K., & Freer, J. (2001). Equifinality, data assimilation, and uncertainty estimation in mechanistic modelling of complex environmental systems using the GLUE methodology. *Journal of Hydrology*, 249(1–4), 11–29. Retrieved from [http://dx.doi.org/10.1016/S0022-1694\(01\)00421-8](http://dx.doi.org/10.1016/S0022-1694(01)00421-8)

Birkel, C., Soulsby, C., Tetzlaff, D., Dunn, S. M., and Spezia, L.: High-frequency storm event isotope $\delta^{18}\text{O}$ sampling reveals time-variant transit time distributions and influence of diurnal cycles, *Hydrol. Process.*, 26, 308–316, DOI:10.1002/hyp.8210, 2012.

Birkel, C., Geris, J., José, M., Mendez, C., Arce, R., Dick, J., Soulsby, C. (2016). Hydroclimatic controls on non-stationary stream water ages in humid tropical catchments. *Journal of Hydrology*. <https://doi.org/10.1016/j.jhydrol.2016.09.006>

Blöschl, G., Bierkens, M. F. P., Chambel, A., Cudennec, C., Destouni, G., Fiori, A., Zhang, Y. (2019). Twenty-three unsolved problems in hydrology (UPH)—a community perspective. *Hydrological Sciences Journal*, 64(10), 1141–1158. <https://doi.org/10.1080/02626667.2019.1620507>

Burns, D. A., Plummer, L. N., McDonnell, J. J., Busenberg, E., Casile, G. C., Kendall, C., ... Schlosser, P. (2003). The Geochemical Evolution of Riparian Ground Water in a Forested Piedmont Catchment. *GroundWater*, 41(7), 913–925. <https://doi.org/10.1111/j.1745-6584.2003.tb02434.x>

Buytaert, W., Deckers, J., & Wyseure, G. (2006). Description and classification of nonallophanic Andosols in south Ecuadorian alpine grasslands (páramo). *Geomorphology*, 73(3–4), 207–221. <https://doi.org/10.1016/j.geomorph.2005.06.012>

Carrillo-Rojas, G., Silva, B., Rollenbeck, R., Céller, R., & Bendix, J. (2019). The breathing of the Andean highlands: Net ecosystem exchange and evapotranspiration over the páramo of southern Ecuador. *Agricultural and Forest Meteorology*, 265(October 2018), 30–47. <https://doi.org/10.1016/j.agrformet.2018.11.006>

Cartwright, I., & Morgenstern, U. (2015). Transit times from rainfall to baseflow in headwater catchments estimated using tritium: The Ovens River, Australia. *Hydrology and Earth System Sciences*, 19(9), 3771–3785. <https://doi.org/10.5194/hess-19-3771-2015>

Cartwright, I., Morgenstern, U., Howcroft, W., Hofmann, H., Armit, R., Stewart, M., Irvine, D. (2020). The variation and controls of mean transit times in Australian headwater catchments. *Hydrological Processes*, 34(21), 4034–4048. <https://doi.org/10.1002/hyp.13862>

Castaño, C., 2002. Páramos y ecosistemas alto andinos de Colombia en condición hotspot & global climatic tensor. Ministerio del Medio Ambiente and Instituto de Hidrología, Meteorología y Estudios Ambientales, Bogotá, Colombia, 387 pp

Coltorti, M., & Ollier, C. D. (2000). Geomorphic and tectonic evolution of the Ecuadorian Andes. *Geomorphology*, 32(1–2), 1–19. [https://doi.org/10.1016/S0169-555X\(99\)00036-7](https://doi.org/10.1016/S0169-555X(99)00036-7)

Córdova, M., Carrillo-Rojas, G., Crespo, P., Wilcox, B., & Céller, R. (2015). Evaluation of the Penman-Monteith (FAO 56 PM) Method for Calculating Reference Evapotranspiration Using Limited Data. *Mountain Research and Development*, 35(3), 230. <https://doi.org/10.1659/mrd-journal-d-14-0024.1>

Córdova, M., Céller, R., Shellito, C. J., Orellana-Alvear, J., Abril, A., & Carrillo-Rojas, G. (2016). Near-surface air temperature lapse rate over complex terrain in the Southern Ecuadorian Andes: Implications for temperature mapping. *Arctic, Antarctic, and Alpine Research*, 48(4), 673–684. <https://doi.org/10.1657/AAAR0015-077>

Correa, A., Breuer, L., Crespo, P., Céller, R., Feyen, J., Birkel, C., Windhorst, D. (2018). SpCorrea, A., Breuer, L., Crespo, P., Céller, R., Feyen, J., Birkel, C., ... Windhorst, D. (2018). Spatially distributed hydro-chemical data with temporally high-resolution

is needed to adequately assess the hydrological functioning of headwater catchments. *Science of The Total Environment*, 651, 1613–1626. <https://doi.org/10.1016/j.scitotenv.2018.09.189>

Correa, A., Ochoa-Tocachi, D., & Birkel, C. (2019). Technical note: Uncertainty in multi-source partitioning using large tracer data sets. *Hydrology and Earth System Sciences*, 23(12), 5059–5068. <https://doi.org/10.5194/hess-23-5059-2019>

Correa, A., Windhorst, D., Tetzlaff, D., Silva, C., Crespo, P., Céller, R., ... Breuer, L. (2017). Spatio-temporal dynamics of runoff sources in Andean Páramo catchments: An event-based approach analysis. *19th EGU General Assembly, EGU2017, Proceedings from the Conference Held 23-28 April, 2017 in Vienna, Austria.*, 19, 1448. Retrieved from <http://adsabs.harvard.edu/abs/2017EGUGA..19.1448C>

Craig, H. (1960). Standard for Reporting Concentrations of Deuterium and Oxygen-18 in Natural Waters. *Science*, 133(1958), 18–19.

Derksen, S., & Keselman, H. J. (1992). Backward, forward and stepwise automated subset selection algorithms: Frequency of obtaining authentic and noise variables. *British Journal of Mathematical and Statistical Psychology*, 45(2), 265–282. <https://doi.org/10.1111/j.2044-8317.1992.tb00992.x>

DeWalle, D. and Edwards, P.: Seasonal isotope hydrology of three Appalachian forest catchments, *Hydrol. Process.*, 11, 1895–1906, 1997

Efron, B. (1983). Estimating the error rate of a prediction rule: improvement on cross-validation. *J. Amer. Statist. Assoc.*, 78(382):316–331

Esquivel-Hernández, G., Mosquera, G. M., Sánchez-Murillo, R., Quesada-Román, A., Birkel, C., Crespo, P., Boll, J. (2019). Moisture transport and seasonal variations in the stable isotopic composition of rainfall in Central American and Andean Páramo during El Niño conditions (2015–2016). *Hydrological Processes*, 33(13), 1802–1817. <https://doi.org/10.1002/hyp.13438>

Gupta, H., Kling, H., Yilmaz, K., & Martinez, G. (2009). Decomposition of the mean squared error and NSE performance criteria: Implications for improving hydrological modelling. *Journal of Hydrology*, 377(1–2), 80–91. <https://doi.org/10.1016/j.jhydrol.2009.08.003>

Heidbüchel, I., Troch, P. A., & Lyon, S. W. (2013). Separating physical and meteorological controls of variable transit times in zero-order catchments. *Water Resources Research*, 49(11), 7644–7657. <https://doi.org/10.1002/2012WR013149>

Hrachowitz, M., Soulsby, C., Tetzlaff, D., Dawson, J. J. C., Dunn, S. M., & Malcolm, I. A. (2009). Using long-term data sets to understand transit times in contrasting headwater catchments. *Journal of Hydrology*, 367(3–4), 237–248.

Hrachowitz, M., Soulsby, C., Tetzlaff, D., & Speed, M. (2009). Catchment transit times and landscape controls—does scale matter? *Hydrological Processes*, 125(June 2009), 1–12. <https://doi.org/10.1002/hyp.7510>

Hrachowitz, M., Soulsby, C., Tetzlaff, D., Malcolm, I. A., and Schoups, G.: Gamma distribution models for transit time estimation in catchments: physical interpretation of parameters and implications for time-variant transit time assessment, *Water Resour. Res.*, 46, W10536, DOI:10.1029/2010WR009148, 10 2010.

Hungerbühler, D., Steinmann, M., Winkler, W., Seward, D., Egüez, A., Peterson, D. E., Hammer, C. (2002). Neogene stratigraphy and Andean geodynamics of southern Ecuador. *Earth-Science Reviews*, 57(1–2), 75–124. [https://doi.org/10.1016/S0012-8252\(01\)00071-X](https://doi.org/10.1016/S0012-8252(01)00071-X)

IAEA. (1997). Isotope in the Study of Environmental Change. In *Isotope Techniques in Th Study of Environmental Change*.

IUSS Working Group WRB. (2015). World Reference Base for Soil Resources 2014, update 2015 International soil classification system for naming soils and creating legends for soil maps. In *World Soil Reports*. <https://doi.org/10.1017/S0014479706394902>

Kirchner, J. (2016a). Aggregation in environmental systems-Part 1: Seasonal tracer cycles quantify young water fractions, but not mean transit times, in spatially heterogeneous catchments. *Hydrology and Earth System Sciences*, 20(1), 279–297. <https://doi.org/10.5194/hess-20-279-2016>

Kirchner, J. (2016b). Aggregation in environmental systems-Part 2: Catchment mean transit times and young water fractions under hydrologic nonstationarity. *Hydrology and Earth System Sciences*, 20(1), 299–328. <https://doi.org/10.5194/hess-20-299-2016>

Kirchner, Tetzlaff, D., & Soulsby, C. (2010). Comparing chloride and water isotopes as hydrological tracers in two Scottish catchments. *Hydrological Processes*, 24(12), 1631–1645. <https://doi.org/10.1002/hyp.7676>

Landon, M., Delin, G., Komor, S., & Regan, C. (2000). Relation of pathways and transit times of recharge water to nitrate concentrations using stable isotopes. *GroundWater* 38, 38(3), 381–395.

Lazo, P., Mosquera, G., McDonnell, J., & Crespo, P. (2019). The role of vegetation, soils, and precipitation on water storage and hydrological services in Andean Páramo catchments. *Journal of Hydrology*, 572(March), 805–819. <https://doi.org/10.1016/j.jhydrol.2019.03.050>

Lin, D., Foster, D. P., & Ungar, L. H. (2011). VIF regression: A fast regression algorithm for large data. *Journal of the American Statistical Association*, 106(493), 232–247. <https://doi.org/10.1198/jasa.2011.tm10113>

Ma, W., & Yamanaka, T. (2013). Temporal variability in mean transit time and transit time distributions assessed by a tracer-aided tank model of a meso-scale catchment. *Hydrological Research Letters*, 7(4), 104–109. <https://doi.org/10.3178/hr.7.104>

Ma, W., & Yamanaka, T. (2016). Factors controlling inter-catchment variation of mean transit time with consideration of temporal variability. *Journal of Hydrology*, 534, 193–204. <https://doi.org/10.1016/j.jhydrol.2015.12.061>

Małoszewski, P., & Zuber, A. (1982). Determining the turnover time of groundwater systems with the aid of environmental tracers. 1. Models and their applicability. *Journal of Hydrology*, 57(3–4), 207–231. [https://doi.org/10.1016/0022-1694\(82\)90147-0](https://doi.org/10.1016/0022-1694(82)90147-0)

Marín, F., Dahik, C. Q., Mosquera, G. M., Feyen, J., Cisneros, P., & Crespo, P. (2018). Changes in soil hydro-physical properties and SOM due to pine afforestation and Grazing in Andean environments cannot be generalized. *Forests*, 10(1). <https://doi.org/10.3390/f10010017>

Mcguire, K., & Mcdonnell, J. (2006). A review and evaluation of catchment transit time modeling. *Journal of Hydrology*, 321, 543–563. <https://doi.org/10.1016/j.jhydrol.2006.04.020>

Montgomery, D., Jennings, C., & Kulahci, M. (2015). *Time Series Analysis and Forecasting* (WILEY, ed.). Hoboken, New Jersey.

Mook, W., & Rozanski, K. (2000). Environmental isotopes in the hydrological cycle. *IAEA Publish*, 39.

Moore, R. D. D. (2004). *Introduction to Salt Streamflow Measurement Part 2: Constant-rate Injection*. 8(1), 12–16.

Mosquera, G. M., Crespo, P., Breuer, L., Feyen, J., & Windhorst, D. (2020). Water transport and tracer mixing in volcanic ash soils at a tropical hillslope: A wet layered sloping sponge. *Hydrological Processes*, 34(9), 2032–2047. <https://doi.org/10.1002/hyp.13733>

Mosquera, Lazo, Céller, Wilcox, & Crespo. (2015). Runoff from tropical alpine grasslands increases with areal extent of wetlands. *Catena*, 125, 120–128. <https://doi.org/10.1016/j.catena.2014.10.010>

Mosquera, Segura, Vaché, Windhorst, Breuer, & Crespo. (2016). Insights into the water mean transit time in a high-elevation tropical ecosystem. *Hydrology and Earth*

Nystrom, U. (1985). Transit Time Distributions of Water in Two Small Forested Catchments. *Ecological Bulletins*, (37), 97–100.

Ochoa-Sánchez, A. E., Crespo, P., Carrillo-Rojas, G., Marín, F., & Céller, R. (2020). Unravelling evapotranspiration controls and components in tropical Andean tussock grasslands. *Hydrological Processes*, 34(9), 2117–2127. <https://doi.org/10.1002/hyp.13716>

Ochoa-Sánchez, Crespo, P., Carrillo-Rojas, G., Sucozhañay, A., & Céller, R. (2019). Actual evapotranspiration in the high andean grasslands: A comparison of measurement and estimation methods. *Frontiers in Earth Science*, 7, 1–16. <https://doi.org/10.3389/feart.2019.00055>

Padrón, R. S., Wilcox, B. P., Crespo, P., & Céller, R. (2015). Rainfall in the Andean Páramo: New Insights from High-Resolution Monitoring in Southern Ecuador. *Journal of Hydrometeorology*, 16(3), 985–996. <https://doi.org/10.1175/jhm-d-14-0135.1>

Penna, D., Stenni, B., Šanda, M., Wrede, S., Bogaard, T. A., Michelini, M., ... Wassenaar, L. I. (2010). Technical note: Evaluation of between-sample memory effects in the analysis of $\delta^{2\text{H}}$ and $\delta^{18\text{O}}$ of water samples measured by laser spectrometers. *Hydrology and Earth System Sciences*, 16(10), 3925–3933. <https://doi.org/10.5194/hess-16-3925-2012>

Peralta-Tapia, A., Soulsby, C., Tetzlaff, D., Sponseller, R., Bishop, K., & Laudon, H. (2016). Hydroclimatic influences on non-stationary transit time distributions in a boreal headwater catchment. *Journal of Hydrology*, 543, 7–16. <https://doi.org/10.1016/j.jhydrol.2016.01.079>

Pham, H. (2019). A new criterion for model selection. *Mathematics*, 7(12), 1–12. <https://doi.org/10.3390/MATH7121215>

Picarro. (2010). ChemCorrectTM - Solving the Problem of Chemical Contaminants in H2O Stable Isotope Research. *White Paper*, 2–4.

Pratt, W. T., Figueroa, J. F., & Flores, B. G. (1997). *Geology and Mineralization of the Area between 3 and 48S. Western Cordillera, Ecuador, British Geological Survey, Open File Report, WCr97r28*.

Quichimbo, P., Tenorio, G., Borja, P., Cárdenas, I., Crespo, P., & Céller, R. (2012). Químicas De Los Suelos Por El Cambio De La Cobertura Vegetal Y Uso Del Suelo : Páramo De Quimsacocha Al Sur Del Ecuador. *Suelos Ecuatoriales*, (February 2014). Retrieved from <https://www.researchgate.net/publication/285632863>

Ramón, Correa, Timbe, Mosquera, Mora, & Crespo. (2021). Do mixing models with different input requirement yield similar streamflow source contributions? Case study: A tropical montane catchment. *Hydrological Processes*, 35(6). <https://doi.org/10.1002/hyp.14209>

Rinaldo, A., Beven, K. J., Bertuzzo, E., Nicotina, L., Davies, J., Fiori, A., Russo, D., and 20 Botter, G.: Catchment travel time distributions and water flow in soils, *Water Resour. Res.*, 47, DOI:10.1029/2011WR010478, 2011.

Renshaw, C. E., Feng, X., Sinclair, K. J., & Dums, R. H. (2003). The use of stream flow routing for direct channel precipitation with isotopically-based hydrograph separations: The role of new water in stormflow generation. *Journal of Hydrology*, 273(1–4), 205–216. [https://doi.org/10.1016/S0022-1694\(02\)00392-X](https://doi.org/10.1016/S0022-1694(02)00392-X)

Santhi, C., Arnold, J. G., Williams, J. R., Dugas, W. A., Srinivasan, R., & Hauck, L. M. (2001). Validation of the SWAT model on a large river basin with point and nonpoint sources. *Journal of the American Water Resources Association*, 37(5), 1169–1188. <https://doi.org/10.1111/j.1752-1688.2001.tb03630.x>

Segura, C., James, A., Lazzati, D., & Roulet, N. (2012). Scaling relationships for event water contributions and transit times in small-forested catchments in Eastern Quebec. *Water Resources Research*, 48(January), 1–21. <https://doi.org/10.1029/2012WR011890>

Siegel, A. (2016). Practical Business Statistics. In ELSEVIER (Ed.), *Urology* (Seven Edit). Seattle: Nikki Levy.

Stewart, M. K., Morgenstern, U., and McDonnell, J. J.: Truncation of stream residence time: how the use of stable isotopes has skewed our concept of streamwater age and origin, *Hydrol. Process.*, 24, 1646–1659, DOI:10.1002/hyp.7576, 2010.

Stockinger, M., Bogena, H., Lücke, A., Diekkrüger, B., Cornelissen, T., & Vereecken, H. (2016). Tracer sampling frequency influences estimates of young water fraction and streamwater transit time distribution. *Journal of Hydrology*, 541, 952–964. <https://doi.org/10.1016/j.jhydrol.2016.08.007>

Stone, M. (1974). Cross-validatory choice and assessment of statistical predictions. *J. Roy. Statist. Soc. Ser. B*, 36:111–147. With discussion by G. A. Barnard, A. C. Atkinson, L. K. Chan, A. P. Dawid, F. Downton, J. Dickey, A. G. Baker, O. Barndorff-Nielsen, D. R. Cox, S. Giesser, D. Hinkley, R. R. Hocking, and A. S. Young

Timbe, E., Windhorst, D., Celleri, R., Timbe, L., Crespo, P., Feyen, J., & Breuer, L. (2015). Sampling frequency trade-offs in the assessment of mean transit times of tropical montane catchment waters under semi-steady-state conditions. *Hydrology and Earth System Sciences*, 1153–1168. <https://doi.org/10.5194/hess-19-1153-2015>

Timbe, E., Windhorst, D., Crespo, P., Feyen, J., Breuer, L., & Use, L. (2014). *Understanding uncertainties when inferring mean transit times of water through tracer-based lumped-parameter models in Andean tropical montane cloud forest catchments*. 1503–1523. <https://doi.org/10.5194/hess-18-1503-2014>

Turner, J., Albrechtsen, H. J., Bonell, M., Duguet, J. P., Harris, B., Meckenstock, R., ... van Lanen, H. (2006). Future trends in transport and fate of diffuse contaminants in catchments, with special emphasis on stable isotope applications. *Hydrological Processes*, 20(1), 205–213. <https://doi.org/10.1002/hyp.6074>

United States Bureau of Reclamation. (2001). *Water Measurement Manual: A Guide to Effective Water Measurement Practices for Better Water Management*.

Van der Hammen, T., H. Hooghiemstra, 2000. Neogene and quaternary history of vegetation, climate and plant diversity in Amazonia. *Quaternary Sci. Rev.*, 19, 725-742

Vittinghoff, E., & McCulloch, C. E. (2007). Relaxing the rule of ten events per variable in logistic and cox regression. *American Journal of Epidemiology*, 165(6), 710–718. <https://doi.org/10.1093/aje/kwk052>

Yu, H., Jiang, S., & Land, K. C. (2015). Multicollinearity in hierarchical linear models. *Social Science Research*, 53, 118–136. <https://doi.org/10.1016/j.ssresearch.2015.04.008>

S. Supplementary material

The supplementary material provides additional information on simple and multiple linear regression models using hydrometeorological variables as predictors for catchments M1-M8. Besides, this auxiliary material includes figures for each catchment in the Zhurucay Ecohydrological Observatory (ZEO). The Pearson correlation coefficients (r) are considered strong when $r \geq 0.50$, moderate when $0.49 \geq r \geq 0.40$, and weak when $r \leq 0.39$. Only the statistically significant results ($p\text{-value} < 0.05$) are displayed.

S1. Simple Linear Regression

The results of the correlations for catchment M6 are shown in Table S1. The Q_{mn} for periods of 1 to 8 months back had a moderate correlation, while Q_{min} had stronger correlations for periods of antecedent conditions, respectively for 3 to 10 months and for a period of yearly MTTs evaluation. The periods with the highest correlations were at 6, 8 and 0+21 months, having a higher correlation (0.71) at 6 and 8 months back, and a correlation of 0.70 at 0+21 months back. No high or significant correlations were found with Q_{mx} . Q_{cum} had a moderate correlation with MTTs for 1 and 8 months of antecedent conditions. Q_{mn} for periods of 2 to 9 months back, and 0+21 and 0+24 months (2 years) back depicted stronger correlations with MTTs. For base flow values (Q_{10} - Q_{30}) weak correlations were found between Q_{10} and MTTs in the 10 to 12 month back conditions. There were low correlations for moderate flow rates (Q_{40} - Q_{60}), and moderate to high correlations for high flow rates (Q_{70} - Q_{90}). Moderate to significant correlations were found for P_{cum} for periods of 0 to 10 months back, and moderately significant for the periods 0+15 to 0+24 back. The highest correlation values were found at 2 and 3 months ($r=0.5$). Moderate to significant correlations were found for P_{mn} for 0 to 10 months back, and 0+15 to 0+24, with the latter correlations being moderately significant; the highest correlation values were found for 2 and 3 months back (0.5). P_{mx} correlations were moderate to significant for periods of 0 to 10 months, and 0+15 to 0+24, with the latter correlations being moderately significant. The highest correlation values were found for 2 and 3 months back (0.5). RC showed weak correlations from 5 to 8 and 12 to 0+21 months back; ET_{cum} moderate negative correlations from 7 to 12 months back; ET_{mn} weak negative correlations from 7 to 9 months back and moderate negative correlations for 10 to 12 months back; and ET_{mx} weak negative correlations for 5, 6, and 0+18 months back, moderate negative correlations for 7 to 9 months back, and strong negative correlations for 10 to 12, 0+21 and 0+24 months back. As for ET_{mn} , weak negative correlations were found for 9 to 12 months back. With ET_{min} , weak correlations were obtained for 0, 6 to 10, and 0+24, and moderate correlations for 1 to 5, 0+15 and 0+21 months back.

Table S 1. Pearson correlation coefficients (r) between the yearly estimated MTTs using a monthly moving window for catchment M6 during the period May 2011 to December 2018, and the hydrometeorological variables for different periods. For the latter, the variables correspond to the median annual value and for the same period the yearly MTTs were estimated (0 months), the median annual values for 1 to 12 months before the period the year MTTs were estimated (1-12 months), and median annual values for the same period the yearly MTTs were estimated adding 3, 6, 9 and 12 months back (0+15-0+24). The values in bold indicate that the r coefficient is higher than 0.5 and statistically significant (p-value <0.05), and underlined values indicate that the r coefficient is lower than 0.5 but statistically significant (p-value <0.05).

Months	Qmn	Qmin	Qmx	Qcum	Qmd	Q ₁₀	Q ₂₀	Q ₃₀	Q ₄₀	Q ₅₀	Q ₆₀	Q ₇₀	Q ₈₀	Q ₉₀	Pmn	Pcum	Pmd	Pmx	RC	ETcum	ETmn	ETmx	ETmd	ETmin
0	0.39	0.20	-0.10	<u>0.38</u>	<u>0.48</u>	0.05	0.04	0.05	0.07	0.13	0.22	<u>0.27</u>	<u>0.33</u>	<u>0.40</u>	<u>0.41</u>	0.38	<u>0.47</u>	<u>-0.25</u>	0.22	0.07	0.09	-0.17	0.19	0.39
1	<u>0.43</u>	0.27	-0.06	<u>0.43</u>	<u>0.49</u>	0.04	0.03	0.04	0.07	0.14	0.22	<u>0.27</u>	<u>0.34</u>	<u>0.41</u>	<u>0.47</u>	<u>0.47</u>	0.50	-0.21	0.22	0.07	0.07	-0.19	0.18	<u>0.46</u>
2	<u>0.43</u>	<u>0.46</u>	-0.11	<u>0.43</u>	0.50	0.07	0.05	0.05	0.09	0.16	<u>0.22</u>	<u>0.28</u>	<u>0.35</u>	<u>0.42</u>	0.51	0.51	<u>0.53</u>	<u>-0.25</u>	0.20	0.07	0.07	-0.21	0.18	<u>0.46</u>
3	<u>0.43</u>	0.59	-0.11	<u>0.43</u>	0.50	0.09	0.07	0.07	0.11	0.19	<u>0.24</u>	<u>0.29</u>	<u>0.37</u>	<u>0.43</u>	0.50	0.50	<u>0.53</u>	<u>-0.25</u>	0.21	0.03	0.03	-0.21	0.14	<u>0.43</u>
4	<u>0.41</u>	0.63	-0.12	<u>0.41</u>	0.50	0.11	0.09	0.09	0.13	0.21	<u>0.25</u>	<u>0.30</u>	<u>0.38</u>	<u>0.44</u>	<u>0.45</u>	<u>0.45</u>	<u>0.48</u>	<u>-0.26</u>	0.21	0.00	0.00	-0.21	0.11	<u>0.41</u>
5	<u>0.44</u>	0.63	-0.12	<u>0.44</u>	0.51	0.14	0.11	0.11	0.16	<u>0.23</u>	<u>0.26</u>	<u>0.31</u>	<u>0.40</u>	<u>0.45</u>	<u>0.46</u>	<u>0.46</u>	<u>0.47</u>	-0.20	<u>0.24</u>	-0.06	-0.07	-0.28	0.05	<u>0.40</u>
6	<u>0.48</u>	0.71	-0.09	<u>0.48</u>	0.57	0.16	0.13	0.12	0.17	<u>0.25</u>	<u>0.27</u>	<u>0.31</u>	<u>0.41</u>	<u>0.46</u>	<u>0.46</u>	<u>0.46</u>	<u>0.48</u>	-0.14	<u>0.29</u>	-0.16	-0.16	-0.36	-0.02	<u>0.35</u>
7	<u>0.49</u>	0.66	-0.03	<u>0.49</u>	0.57	0.18	0.14	0.13	0.19	<u>0.26</u>	<u>0.28</u>	<u>0.31</u>	<u>0.42</u>	<u>0.48</u>	<u>0.45</u>	<u>0.45</u>	<u>0.43</u>	-0.07	<u>0.33</u>	<u>-0.22</u>	<u>-0.23</u>	<u>-0.41</u>	-0.09	<u>0.31</u>
8	0.46	0.71	0.00	0.46	0.55	0.20	0.16	0.15	0.20	0.28	0.29	0.32	0.44	0.50	0.42	0.42	0.38	-0.01	0.30	-0.30	-0.31	-0.46	-0.18	0.27
9	<u>0.39</u>	0.68	0.02	<u>0.39</u>	0.50	0.23	0.17	0.17	0.22	<u>0.29</u>	<u>0.30</u>	<u>0.33</u>	<u>0.46</u>	0.52	<u>0.37</u>	<u>0.37</u>	<u>0.35</u>	0.00	0.22	<u>-0.35</u>	<u>-0.38</u>	<u>-0.49</u>	<u>-0.28</u>	<u>0.25</u>
10	0.22	0.61	0.02	0.22	<u>0.38</u>	<u>0.26</u>	0.19	0.19	<u>0.24</u>	<u>0.31</u>	<u>0.31</u>	<u>0.34</u>	<u>0.48</u>	0.54	<u>0.27</u>	<u>0.27</u>	<u>0.25</u>	0.02	0.04	<u>-0.37</u>	<u>-0.40</u>	-0.52	<u>-0.33</u>	<u>0.20</u>
11	-0.01	<u>0.46</u>	-0.02	-0.01	0.20	<u>0.28</u>	0.21	0.20	<u>0.25</u>	<u>0.32</u>	<u>0.32</u>	<u>0.34</u>	<u>0.49</u>	0.55	0.11	0.11	0.14	-0.01	-0.16	<u>-0.38</u>	<u>-0.41</u>	-0.52	<u>-0.37</u>	0.18
12	-0.21	0.27	-0.03	-0.21	0.01	<u>0.32</u>	0.24	0.22	<u>0.27</u>	<u>0.34</u>	<u>0.33</u>	<u>0.36</u>	0.51	0.55	-0.05	-0.05	-0.03	-0.07	<u>0.30</u>	<u>-0.38</u>	<u>-0.42</u>	-0.50	<u>-0.36</u>	0.14
0+15	<u>0.35</u>	0.40	0.00	<u>0.35</u>	0.38	-0.02	-0.03	-0.03	0.02	0.11	0.19	<u>0.25</u>	<u>0.33</u>	<u>0.42</u>	<u>0.34</u>	<u>0.34</u>	<u>0.34</u>	<u>-0.31</u>	<u>0.29</u>	-0.10	0.06	-0.19	0.15	<u>0.43</u>
0+18	0.30	0.55	-0.05	<u>0.30</u>	0.40	0.07	0.05	0.06	0.10	0.18	0.24	<u>0.29</u>	<u>0.37</u>	<u>0.44</u>	<u>0.27</u>	<u>0.27</u>	<u>0.33</u>	<u>-0.29</u>	<u>0.31</u>	-0.15	-0.06	<u>-0.36</u>	0.04	<u>0.40</u>
0+21	<u>0.35</u>	0.70	-0.09	<u>0.35</u>	0.56	0.18	0.14	0.14	0.18	0.25	<u>0.30</u>	<u>0.34</u>	<u>0.41</u>	<u>0.47</u>	0.34	<u>0.34</u>	<u>0.46</u>	<u>-0.27</u>	<u>0.30</u>	-0.11	-0.17	-0.55	-0.06	<u>0.43</u>
0+24	0.15	0.40	-0.21	0.15	<u>0.55</u>	0.27	0.23	0.23	0.26	0.33	0.37	0.40	0.47	0.50	0.26	0.26	0.47	<u>-0.31</u>	-0.02	-0.04	-0.19	-0.64	-0.08	0.39

Abbreviations: **Qmn** mean streamflow; **Qmin** minimum streamflow; **Qmx** maximum streamflow; **Qcum** accumulated streamflow; **Qmd** median streamflow; **Q₁₀, Q₂₀, Q₃₀...Q₉₀** streamflow rates as the frequency of non-exceedance. **Pmn** mean precipitation; **Pcum** accumulated precipitation; **Pmd** median precipitation; **Pmx** maximum precipitation; **RC** runoff coefficient; **RHmn** relative humidity; **SRmx** maximum solar radiation; **SRmin** minimum solar radiation; **Tmin** minimum temperature; **WSmx** maximum wind speed; **ETcum** accumulated evapotranspiration; **ETmn** mean evapotranspiration; **ETmx** maximum evapotranspiration; **ETmd** median evapotranspiration; **ETmin** minimum evapotranspiration.

UCUENCA

The results of the Pearson correlation (r) between hydro-meteorological variables and MTTs for the remaining catchments are presented in Figure S1, and it was found that Qmd (Fig. S1.a), Pmd (Fig. S1.b), and ETmx (Fig. S1.c) influence MTTs.

The catchment M1 had correlations with MTTs larger than 0.5 for 5 to 6 months back, stronger correlations between Pmd and MTTs were found for 0 to 6 months of antecedent conditions. ETmx had stronger correlations for 0+21 to 0+24 antecedent conditions, moderate correlations for 8 to 12 months back and weak correlations for the rest. For the M2 catchment, Qmd had only moderate correlations and the maximum correlation was 0.48 for 7-8 months back. Most of the correlations were significant, except for 11 to 0+15. Stronger correlations with Pmn were found for 0 to 2 months of antecedent conditions, while weak negative correlations with ETmx, but not for the others. The M3 catchment had stronger correlations with Qmd from 6 to 11 months, with 0.69 being the highest at 10 months. Moderate correlations between Pmd and MTTs were found for 0 to 3 months back, and a strong correlation for the 0+24 months back. Instead, ETmax had stronger correlations between months 9 to 12, and 0+21 and 0+24. For catchment M4, Qmd had stronger correlations for 6 to 7, and 0+24 months back, and Pmd for 1 to 3 and 0+24 months back. The correlations between ETmx and MTTs were weak for 5 to 7 months and 0+18, moderate for months 8 to 9 months back, and strong for months 10 to 12 and 0+24 months back. In catchment M5, Qmd had stronger correlations for 0+21 and 0+24. For Pmd there were no correlations greater than 0.5, however, the highest correlation was -0.38 for 12 months. ETmx had weak correlations from 0 to 1 months, the rest of the correlations were not significant. For the M7 catchment, Qmd had weak correlations from 7 to 0+15 months back. However, there were no correlations of MTTs with Pmd higher than 0.5, the highest value of correlation was 0.42 for 12 months back. ETmx had moderate correlations from 8 to 11 and 0+24 months back. In the M8 catchment, Qmd obtained strong correlations from 1 to 7 months antecedent conditions. However, for Pmd only weak correlations were observed from 0 to 3 months back. ETmx had weak correlations from 1 to 6 months and 0+18 months, moderate correlations from 7 to 12 months, and strong correlations for the periods 0+21 and 0+24.

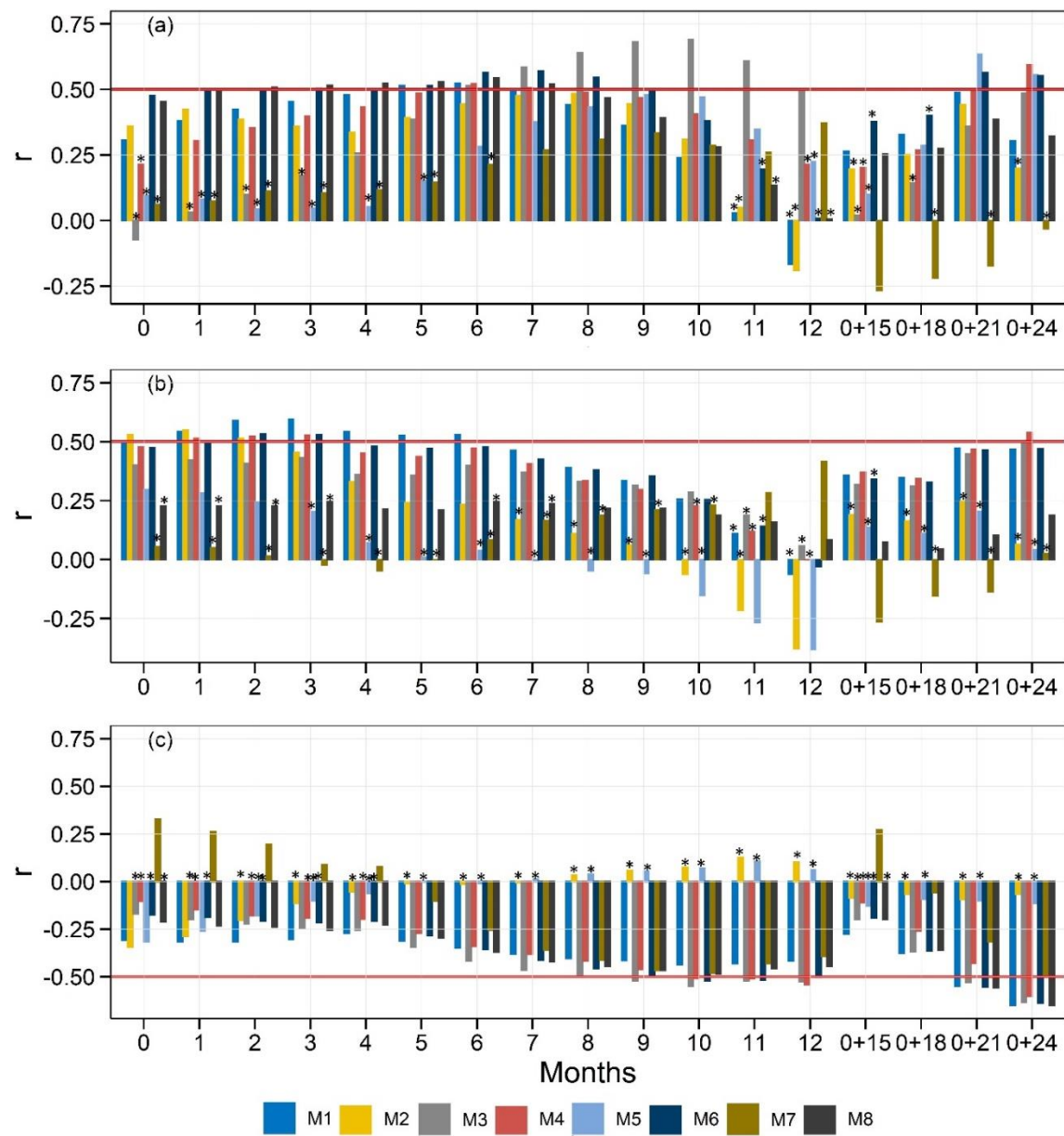


Figure S 1. Pearson correlation coefficients (r) between the yearly estimated MTTs using a monthly moving window for the catchments M1-M8 during the period May 2011 - December 2018; subplot (a) median streamflow; (b) median precipitation and (c) maximum evapotranspiration for the periods shown in the x-axis. The streamflow, precipitation, and evapotranspiration variables correspond to the mean annual values for the same period the yearly MTTs were estimated (0 months), the mean annual values for 1 to 12 months before the period the year MTTs were estimated (1-12 months), and mean annual values for the same period the yearly MTTs were estimated adding 3, 6, 9 and 12 months back (0+15...0+24). The horizontal red lines depicts for reference the r -value of 0.5. The asterisks represent non significative correlations (p -value < 0.05).

S2. Multiple Linear Regressions

In all the multiple linear regression models 57 observations were used for the catchments M1-M8. The variables and the results for each of the catchments are detailed below.

In the linear regression analysis for catchment M1, a total of 8 variables were used, respectively Q_{mx_2} , P_{mx_7} , Q_{md_8} , $Q_{min_{0+15}}$, $P_{cum_{0+18}}$, $Q_{min_{24}}$, ET_{min_0} , and P_{cum_0} . Subsequently, MLRs were performed, and 5 models were obtained. Figure S2.1. shows all the derived models, and model A2 was selected as representative for this catchment.

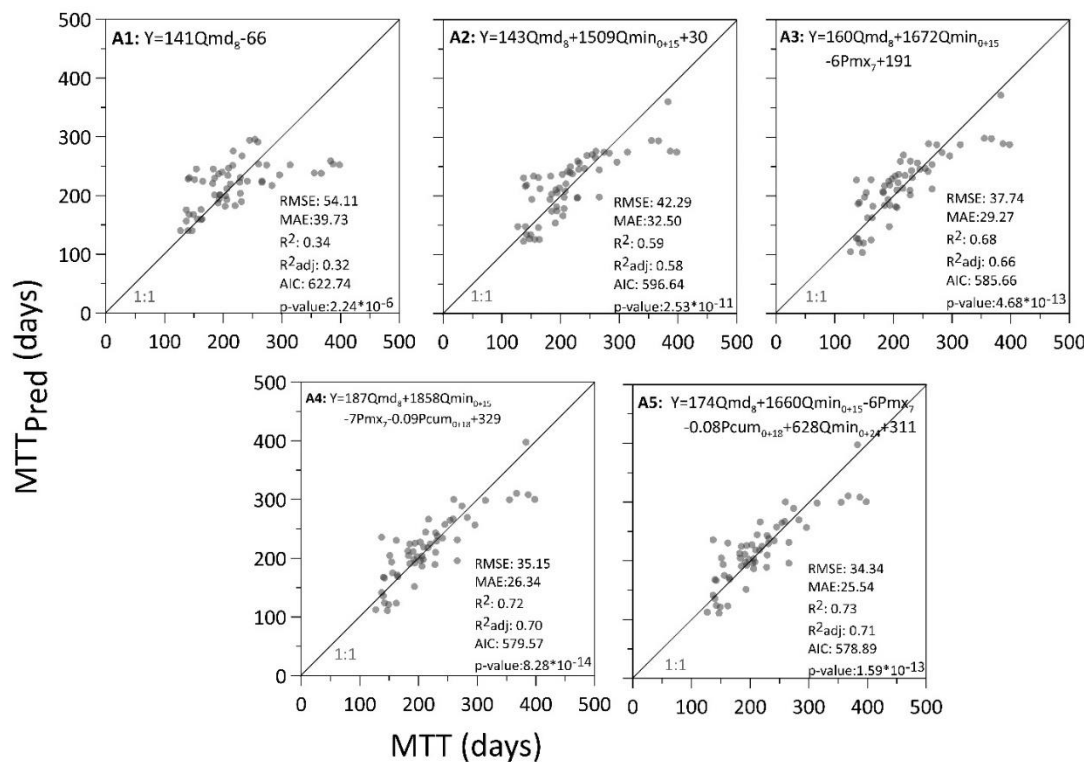


Figure S2. 1. Multiple linear regression models for catchment M1 for the period May 2011 to December 2018 using hydro-meteorological variables as predictors. **A1** to **A5** represent different models after incorporating explanatory variables. The number next to the hydrological variable indicates the corresponding moving window. Abbreviations: **Qmd** median streamflow; **Qmin** minimum streamflow; **Pmx** maximum precipitation; **Pcum** accumulated precipitation. The dashed line corresponds to the linear regression and the gray line corresponds to the 1:1 ratio.

In the linear regression analysis for catchment M2, a total of 10 variables were used: Q_{min_0} , P_{mx_0} , P_{cum_0} , Q_{mx_1} , RC_8 , $Q_{min_{10}}$, $Q_{acum_{0+18}}$, RC_{0+21} , RC_{0+24} , RC_{0+24} , and ET_{min_6} . MLRs were performed and 4 models obtained. Figure S2.2.

shows all the derived models, and model A2 was selected as representative for this catchment.

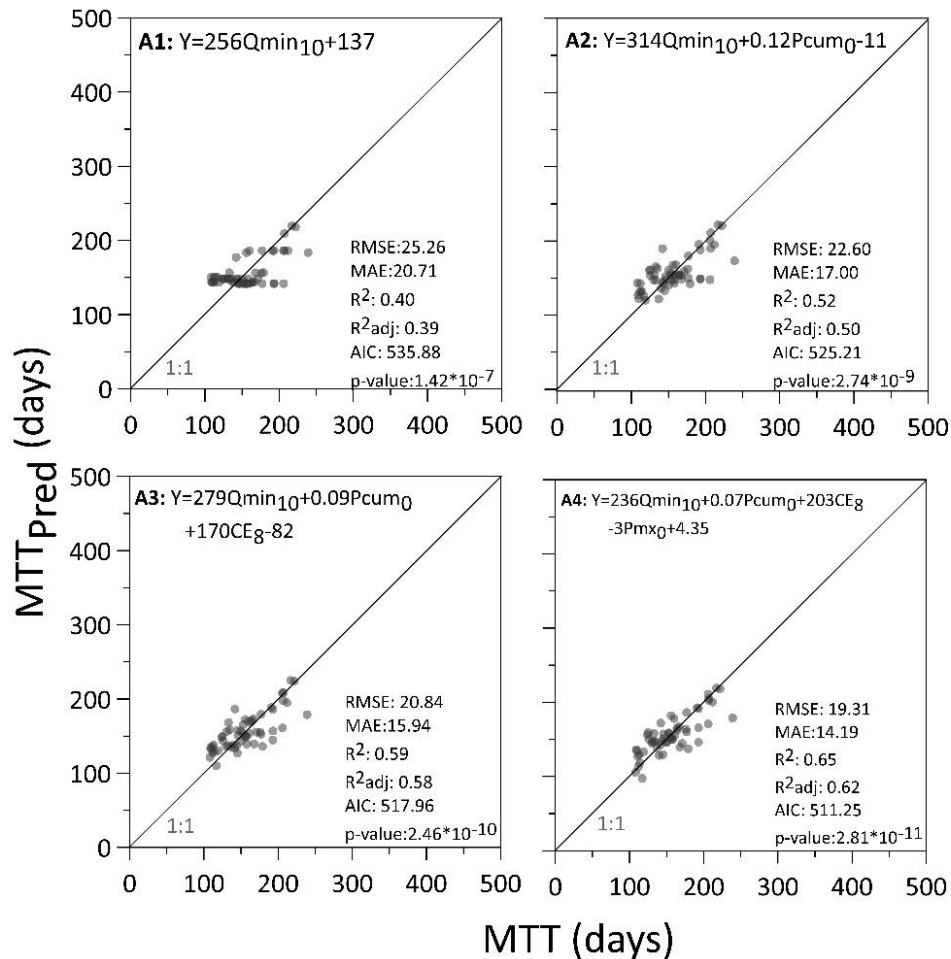


Figure S2. 2. Multiple linear regression models for catchment M2 during the period May 2011 to December 2018 using hydro-meteorological variables as predictors. **A1** to **A4** represents different models after incorporating explanatory variables. The number next to the hydrological variable indicates the corresponding moving window. Abbreviations: **Qmin** minimum streamflow; **RC** runoff coefficient; **Pmx** maximum precipitation; **Pcum** accumulated precipitation. The dashed line corresponds to the linear regression and the gray line corresponds to the 1:1 ratio.

In the linear regression analysis for catchment M3, a total of 8 variables were used: $Pcum_0$, Qmd_7 , $Qmin_{11}$, $Pcum_{0+18}$, $Q30_{0+18}$, RC_{0+18} , $ETmx_3$, and $ETmin_6$. MLRs were performed and 5 models obtained. Figure S2.3. shows all the derived models, and model A2 was selected as representative for this catchment.

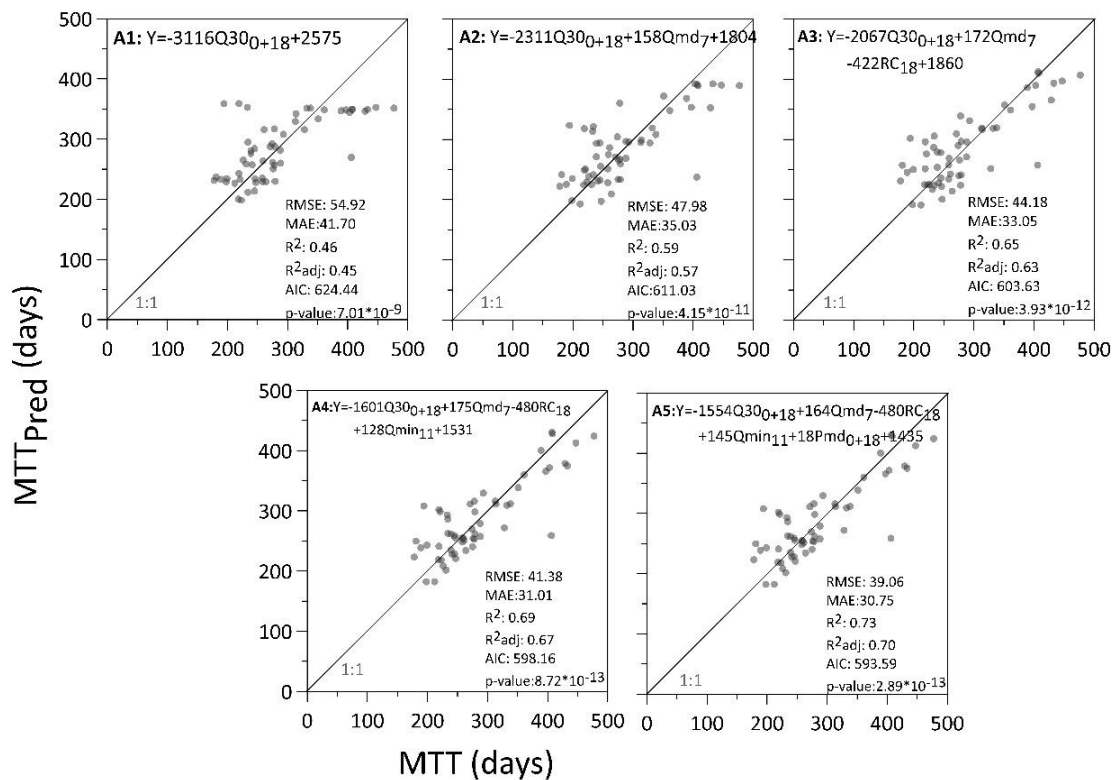


Figure S2.3. Multiple linear regression models for catchment M3 during the period May 2011 to December 2018 using hydro-meteorological variables as predictors. **A1** to **A5** represents different models after incorporating explanatory variables. The number next to the hydrological variable indicates the corresponding moving window. Abbreviations. Abbreviations: **Q₃₀** streamflow rates as the frequency of non-exceedance; **Q_{md}** median streamflow; **RC** runoff coefficient; **Q_{min}** minimum streamflow; **P_{md}** median precipitation. The dashed line corresponds to the linear regression and the gray line corresponds to the 1:1 ratio.

In the linear regression analysis for catchment M4, a total of 9 variables were used: $Pcum_0$, RC_3 , Qmx_7 , RC_9 , RC_{0+18} , $Qcum_{0+24}$, RC_{0+24} , $ETmx_{0+18}$, $Etomx_{12}$, and $Q30_{0+18}$. MLRs were performed and 4 models obtained. Figure S2.4. shows all the derived models, and model A3 was selected as representative for this catchment.

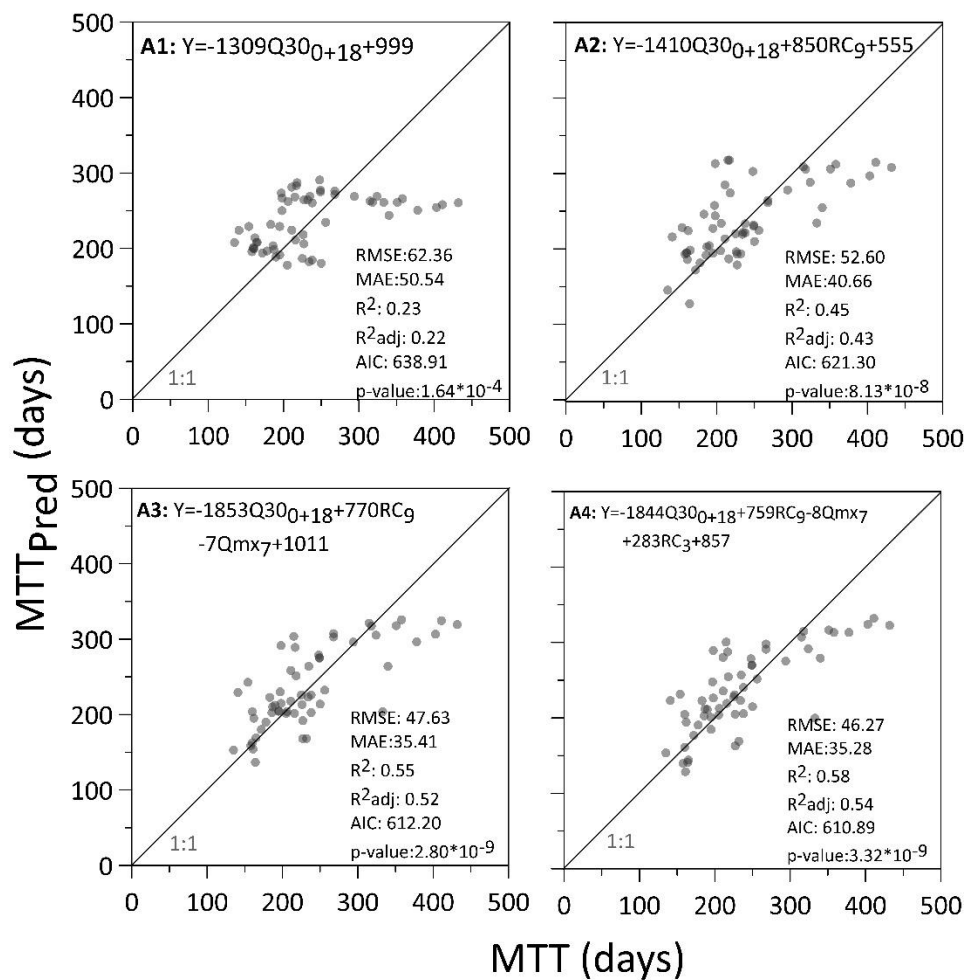


Figure S2.4. Multiple linear regression models for catchment M4 during the period May 2011 to December 2018 using hydro-meteorological variables as predictors. A1 to A4 represents different models after incorporating explanatory variables. The number next to the hydrological variable indicates the corresponding moving window. Abbreviations. **Q₃₀** streamflow rates as the frequency of non-exceedance; **RC** runoff coefficient; **Q_{mx}** maximum streamflow. The dashed line corresponds to the linear regression and the gray line corresponds to the 1:1 ratio.

In the linear regression analysis for catchment M5, a total of 9 variables were used: $Q_{cum,0+24}$, RC_3 , $Q_{min,9}$, $Q_{cum,9}$, $Q_{md,12}$, $P_{mx,12}$, $Q_{cum,0+18}$, RC_{0+21} , and $ET_{min,0}$. MLRs were performed and 5 models obtained. Figure S2.5. shows all the derived models, and model A4 was selected as representative for this catchment.

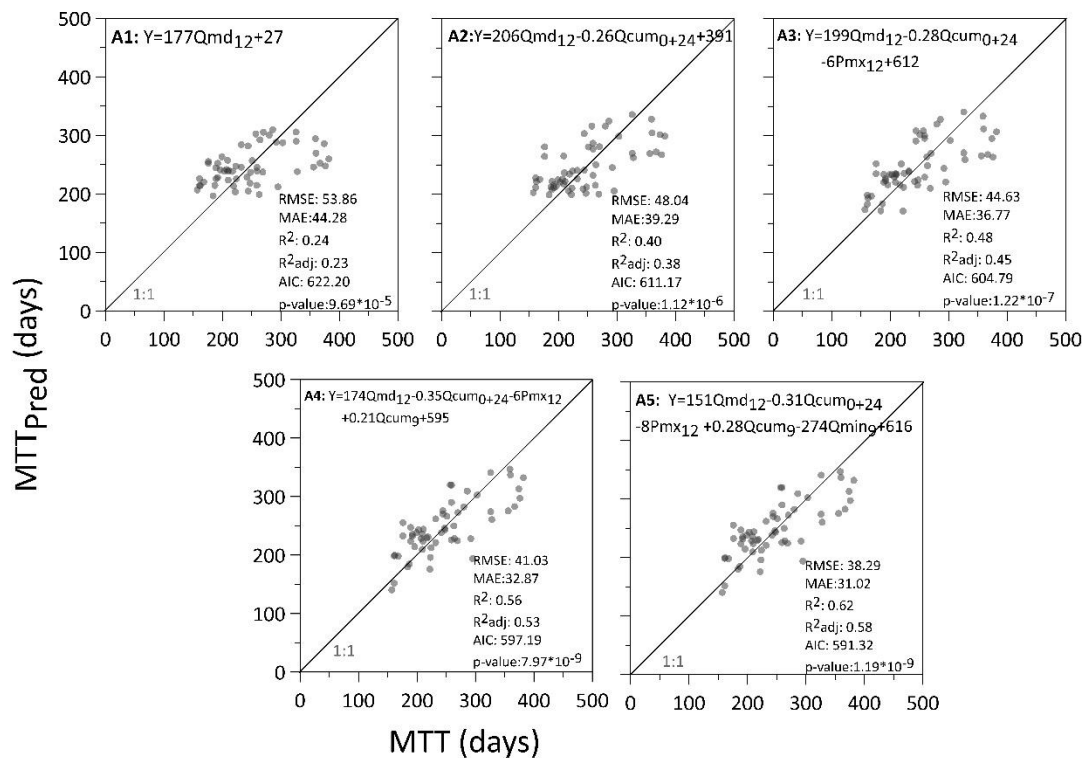


Figure S2.5. Multiple linear regression models for catchment M5 during the period May 2011 to December 2018 using hydro-meteorological variables as predictors. **A1** to **A5** represents different models after incorporating explanatory variables. The number next to the hydrological variable indicates the corresponding moving window. Abbreviations: **Qmd** median streamflow; **Qcum** accumulated streamflow; **Pmx** maximum precipitation; **Qmin** minimum streamflow. The dashed line corresponds to the linear regression and the gray line corresponds to the 1:1 ratio.

In the linear regression analysis for catchment M8, a total of 11 variables were used: Q_{cum0} , Q_{min3} , Q_{min12} , Q_{mx12} , $Q_{cum0+18}$, ET_{min0} , P_{md8} , P_{md10} , P_{mx12} , P_{md12} , and P_{mx9} . MLRs were performed and 5 models obtained. Figure S2.6. shows all the derived models, and model A5 was selected as representative for this catchment.

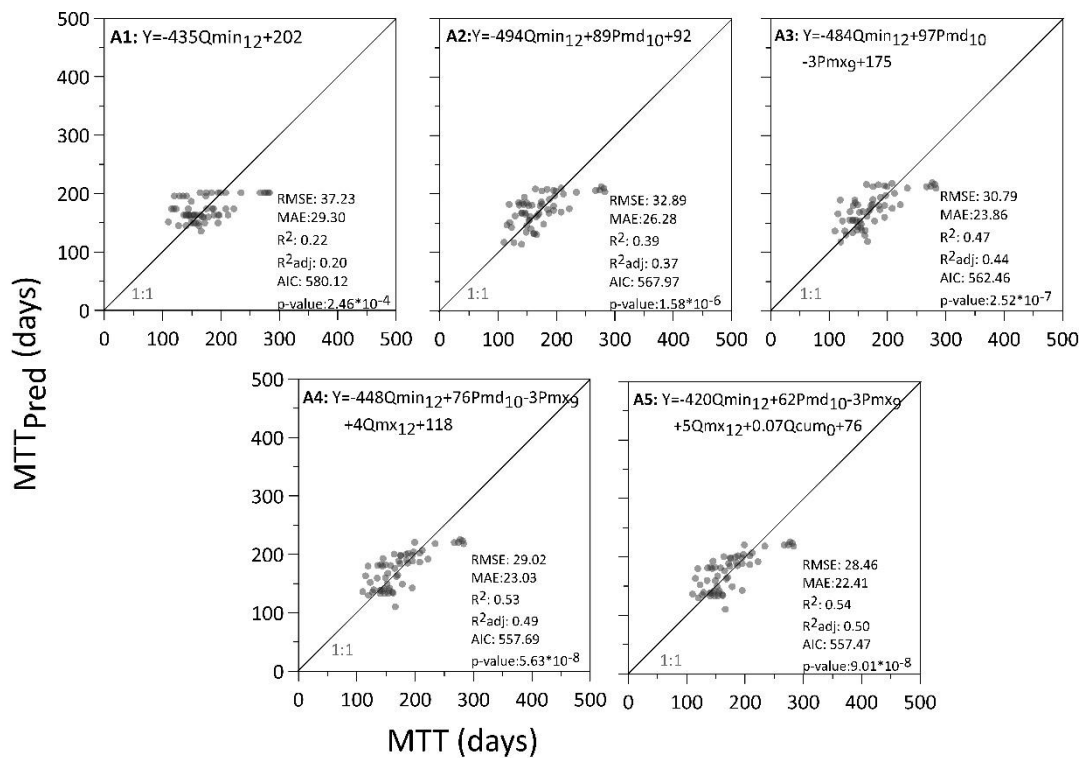


Figure S2.6. Multiple linear regression models for catchment M8 during the period May 2011 to December 2018 using hydro-meteorological variables as predictors. A1 to A5 represents different models after incorporating explanatory variables. The number next to the hydrological variable indicates the corresponding moving window. Abbreviations: **Qmin** minimum streamflow; **Pmd** median precipitation; **Pmx** maximum precipitation; **Qmx** maximum streamflow; **Qcum** accumulated streamflow. i.eThe dashed line corresponds to the linear regression and the gray line corresponds to the 1:1 ratio.